d·Collection

Intrinsic network abnormalities and effects of oxytocin receptor gene in children with autism spectrum disorder

자폐스펙트럼장애 아동의 내재적 뇌 네트워크 이상과 옥시토신수용체의 영향

August 2023

Graduate School of Medicine
Seoul National University
Neuropsychiatry Major

Narae Yoon

Intrinsic network abnormalities and effects of oxytocin receptor gene in children with autism spectrum disorder

지도교수 김 붕 년

이 논문을 의학박사 학위논문으로 제출함

2023년 4월

서울대학교 대학원

의학과 정신과학 전공

윤 나 래

윤나래의 박사 학위논문을 인준함

2023년 7월

위 원 장	_____	(인)
부위원장	_____	(인)
위　　원	_____	(인)
위　　원	_____	(인)
위　　원	_____	(인)

Abstract

Background: The oxytocin receptor gene (OXTR) has been shown to be associated with several characteristics of autism spectrum disorder (ASD). Aberrant intrinsic brain network is a consistent finding in ASD and recent studies have suggested that OXTR may impact the brain functional networks of ASD. However, the strength of functional connectivity (FC) across brain regions has yielded mixed results and little is known about the relationship between OXTR and FC in ASD especially in younger children. In this study, we investigated the FC of the resting brain in children with low-functioning ASD, including children in the early developmental stage. Next, we explored the effects of OXTR on FC patterns typically observed in children with ASD. The relationship between clinical symptoms of ASD and FC associated with OXTR was investigated together.

Methods: A total of 43 children with ASD and 54 typically developing (TD) children aged between 2 and 12 years were participated in the study. Through blood tests, we acquired genotype data for two single-nucleotide polymorphisms (SNPs) of the OXTR gene (rs2254298 and rs53576), as well as DNA methylation data for two CpG sites (-924 and -934), from the participants. In addition, we collected brain imaging data using resting-state functional magnetic resonance imaging. We employed independent component analysis to categorize the brain regions into six intrinsic networks and evaluated the FC of each network. Afterward, we examined the interaction effect of the OXTR and diagnosis on the FCs. Finally, we tested the correlation between aberrant FCs associated with OXTR and clinical symptom scores of autism.

Results: The results of the comparison of FC between the ASD children and TD children were as follows. The under-connectivities within several brain networks, including the cognitive control network, default mode network, visual (VIS) network, and somatomotor (SM) network, were observed in children with ASD. In contrary, we found over-connectivities in children with ASD compared with TD children between the subcortical, VIS, and SM networks. These networks were significantly correlated with the clinical scores of ASD. In the imaging genetic analysis on the OXTR, the following outcomes were obtained. With respect to the risk allele of both SNPs (rs2254298 and rs53576), we found the decreased FCs in ASD and the increased FCs in TD in most of the intrinsic brain networks. As a consequence, the differences between the FCs of two groups were significantly amplified. On the contrary, in some FCs related to subcortico-cortical networks, an increase in connectivity was observed in ASD, while a decrease was observed in TD. Therefore, the contrast between the two groups became more pronounced, as in the previous findings. We found significant correlations between the FC values and the ADOS Calibrated Severity Scores. In the imaging epigenetic analysis of the OXTR, we observed that the increase in methylation level of the two CpG sites (-924 and -934) had a significant effect on the difference in the FCs between the two groups. No clinical correlation was found here. Finally, the results of spectral analysis to see fluctuations in intrinsic connectivity were as follows. The TD group showed greater power in low-frequency bands than the ASD group, and the ASD group showed greater power in high-frequency bands than the TD group. Findings from spectra power analysis related to OXTR were also observed in similar directions. However, the spectral power according to the genotype of OXTR was significant only at low

frequencies, and the TD group showed greater power than the ASD group. The results according to the methylation level of OXTR were the same as the previous group comparison in one independent component (SM).

Conclusions: The results of this study indicate that the resting brain networks develop in various directions depending on the brain regions of children with ASD, and this aberrant intrinsic connectivity, which differs significantly from TD children, is likely to be a biological basis for the diagnosis of autism. In addition, the consistent effect of genetic and epigenetic variations in the OXTR gene on differences in intergroup FC across various brain regions implies the potential use of imaging genetics/epigenetics of OXTR as a biomarker for ASD.

Keywords: Autism spectrum disorder, oxytocin receptor gene, imaging genetics, imaging epigenetics, resting-state functional MRI, independent component analysis
Student Number: 2017-34954

Table of Contents

Figures

Tables

List of Abbreviations

ACC   anterior cingulate cortex

ACG   anterior cingulate gyrus

ADOS   Autism Diagnostic Observation Schedule

ASD   autism spectrum disorder

AUD   auditory network

CARS   Childhood Autism Rating Scale

CC   cognitive control network

CG   cingulate gyrus

CSS   calibrated severity score

DMN   default mode network

FC   functional connectivity

FDR   false discovery rate

FNC   functional network connectivity

FSIQ   full scale intelligence quotient

FWE   family-wise error

EPI   echo planar imaging

IC   independent component

ICA   independent component analysis

IPL   inferior parietal lobule

MNI   Montreal Neurological Institute

mPFC   medial prefrontal cortex

NAcc   nucleus accumbens

OXTR   oxytocin receptor gene

PCC   posterior cingulate cortex

PCR   polymerase chain reaction

rs FC   resting-state functional connectivity

rs-fMRI   resting-state functional magnetic resonance imaging

SCI   Social Communication and Interaction

SD   standard deviation

SM   somatomotor network

SNP   single-nucleotide polymorphism

SPL   superior parietal lobule

SRS   Social Responsiveness Scale

SUB   subcortical network

TC   time course

TD   typically developing

VIS   visual network

Introduction

Study Background

Autism spectrum disorder (ASD) has a complex etiology in which the development of the brain network is disturbed by the interaction between genes and the environment (1, 2). Although ASD is heritable, its specific pathogenesis has not been identified, and biomarkers related to its specific neural system are not yet determined. Therefore, establishing the diagnosis of ASD remains phenomenological, which is based on children's developmental histories and observations of clinical symptoms (3). However, as individuals with ASD show a significantly wide range of symptoms and severities, the diagnosis can be remarkably complex, leading to delayed diagnosis or misdiagnosis (3, 4).

Several studies on the biomarkers of ASD have been conducted (2), and brain imaging is a promising biomarker candidate because of the neural underpinnings of ASD (5, 6). In particular, resting-state functional magnetic resonance imaging (rs-fMRI) has been widely studied to measure intrinsic functional connectivity (FC) (7-9). As rs-fMRI data can be acquired without performing tasks in a relatively short scanning time, it has the advantage of obtaining data from participants with functional difficulties, such as ASD (10). Therefore, rs-fMRI has been extensively examined in individuals with ASD, and previous studies using rs-fMRI have shown evidence of the alterations in functional brain networks in ASD (10-12).

However, findings on intrinsic FC patterns have been inconsistent (11). In a review paper published in 2013, Uddin et al. found increased FC in several brain

networks in young children with ASD, but opposite findings were observed in adolescents and adults with ASD (13). They emphasized the importance of the developmental perspective in autism neuroimaging studies. In addition to developmental factors, differences in neuroimaging methodologies can affect FC outcomes. Nair et al. reported that they observed significant effects for some methodological factors, such as type of analysis, field of view, and dataset (14). They suggested that the combination of different methodological approaches could contribute to the understanding of the FC of ASD (14, 15). Recent evidence from studies of intrinsic FC implies pervasive alterations of the brain network with combined connectivity patterns of both over- and under-connectivities (16). Although developmental and methodological factors have been discussed, the inconsistency of connectivity patterns in ASD has not been clearly explained. Additionally, as ASD has a remarkably wide spectrum of symptoms and severities, this effect on FC cannot be ruled out.

Independent component analysis (ICA) is a data-driven method that makes the analysis of connectivity easier and applicable to the whole brain. This method does not need to define a prior region and is well-suited for analyzing rs-fMRI data. Previous studies using ICA have also found abnormal FC in patients with ASD (17-20). For example, Braden et al. (2017) studied men aged 40–64 years with ASD and found reduced engagement of the cortico-striatal-thalamic-cortical neural network. They also reported that men with ASD had less activity in brain networks that allowed for flexible thinking than men in general (17). Wang et al. (2019) demonstrated that dysfunction of the default mode network (DMN) was a key feature in the co-occurrence of ASD and attention deficit hyperactivity disorder,

including connectivities within the DMN and between the default mode and somatomotor (SM) networks (19). However, until now, few studies have been conducted on low-functioning children with severe ASD with regard to FC.

The oxytocin system, which is involved in social functioning including social cognition, social bonding, and stress regulation (21-23), has been implicated in the etiology of ASD and it has been frequently reported that individuals with ASD commonly possess genetic polymorphisms of oxytocin receptor gene (OXTR) (24-26). The OXTR gene has multiple single nucleotide polymorphisms (SNPs) that have been investigated in relation to ASD (27). A meta-analysis by LoParo and Waldman (2015) (28) found that several OXTR gene variants were significantly associated with ASD, including rs7632287, rs237887, rs2268491 and rs2254298. Another meta-analysis in 2016, the authors confirmed these findings and identified several other OXTR gene variants that were associated with ASD (25). Furthermore, the authors found that the genetic variations were also shown to be associated with clinical symptoms of ASD.

In addition, imaging genetic studies have investigated the relationship between OXTR polymorphisms and brain function and structure in ASD, and the most abundant findings were observed for polymorphisms of two SNPs, rs2254298 and rs53576. A previous study found that individuals who carried the rs53576 A allele of OXTR showed reduced volume of hypothalamus and decreased amygdala reactivity to emotional processing (29). Another study reported that the presence of rs53576 G allele in OXTR was linked to higher neural activity related to mentalizing in both temporal poles and precunei (30). It has been reported that the risk allele (A allele) of rs2254298 was associated with increased amygdala volume,

3

and decreased hypothalatmus, anterior cingulate cortex(ACC), and insula, and deactivation of ACC in previous structural MRI and fMRI studies (31-34). However, most previous research was conducted with healthy adults as subjects, and the brain regions of interest in earlier studies were limited to areas where oxytocin receptors are expected to be distributed densely, such as limbic and ventral forebrain including nucleus accumbens (NAcc), hypothalamus and amygdala (35). Therefore, in this study, we aimed to explore the effects of the genetic polymorphisms of these two SNPs (rs2254298 and rs53576) on the intrinsic functional networks of the entire brain of children with severe ASD.

Recently, studies on the effects of epigenetics of OXTR, as well as genetics, have been carried out in ASD. Epigenetic modifications such as DNA methylation can regulate gene expression and a growing body of research has focused on investigating epigenetic modifications of OXTR in individuals with ASD. DNA methylation is involved in regulating transcription of the gene and generally associated with a decrease in gene transcription leading to reduced expression of the respective protein (36). Previous review articles addressed DNA methylation of OXTR and social behavior in relation to the characteristics of ASD (37, 38). In a systematic review, authors reported that OXTR hypermethylation was associated with autistic traits in adults and decreased brain FC between the superior temporal sulcus and posterior cingulate cortex (PCC) (36). These findings suggest that epigenetic modifications of OXTR may be involved in the etiology of ASD and may have potential diagnostic and therapeutic implications. DNA methylation occurs in cytosines of CpG dinucleotides, and DNA regions where CpG dinucleotides are enriched are called CpG islands (39). Among the CpG sites of

OXTR, CpG sites -924 and -934 have been reported to be more methylated in individuals with ASD (36, 40). In this study, we explored the effects of hypermethylation of these two CpG sites on FC of the whole brain networks in children with ASD.

Purpose of Research

In this study, we aimed to investigate the characteristics of resting brain FC in children with severe ASD that are distinct from those in typically developing (TD) children and to explore the effect of the OXTR on aberrant connectivity using rs-fMRI. First, we compared the overall brain connectivity of ASD children and those of TD children to discover the types of networks showing abnormalities in children of autism. Using various analysis methods of ICA, we tried to identify the brain regions where abnormalities were repeatedly found with different measurements. Next, we explored the difference between the ASD children and the TD children in the abnormality of resting brain FC according to the genotype of the OXTR. As mentioned above, we aimed to search the entire brain regions in our imaging genetic analysis, not limiting the region of interest to oxytocin-related areas. Finally, we examined how the aberrant resting brain connectivity of the two groups changed according to the DNA methylation of the OXTR. Imaging epigenetic analysis was also performed for the whole brain region in the same way as imaging genetics.

In this study, our hypotheses were as follows. First, there would be significant differences in resting brain FC between ASD and TD children, and the differences would appear in various directions showing over- or under-connectivity depending

on the brain area, not in the same way. Second, genetic and epigenetic variances in OXTR would influence the abnormal resting brain FC found in children with ASD. Recessive genotypes of OXTR would exacerbate aberrant network connectivities, and hypermethylation of OXTR would similarly aggravate the abnormalities. Third, the genetic and epigenetic imaging results of OXTR would show significant correlations with the clinical symptoms and phenotypes of ASD.

Considering the insufficient studies on FC in children with ASD with severe symptoms at a younger age including preschoolers, especially the lack of genetic and epigenetic imaging studies of the OXTR targeting ASD children, we expected that this study would yield meaningful results for the research on biomarkers in ASD.

Methods

Participants

In total, 43 children with ASD and 54 TD children aged between 2 and 12 years were included in this study. They were recruited from Seoul National University Hospital (SNUH) in Seoul, South Korea, between October 2015 and March 2021. All the children with ASD were medication-naïve and diagnosed by board-certified child and adolescent psychiatrists based on the diagnostic criteria of the Diagnostic and Statistical Manual, 5th edition. The exclusion criteria for the ASD group were as follows: hereditary genetic disorder; current or past history of brain trauma, organic brain disorder, seizure, or any neurological disorder; schizophrenia or any other childhood-onset psychotic disorder; major depressive disorder or bipolar disorder; Tourette's syndrome or a chronic motor/vocal tic disorder; and obsessive-compulsive disorder. The control group included TD children who had never been diagnosed with psychiatric disorders, and the same exclusion criteria for the ASD group were applied to the TD group with the additional exclusion criterion of an ASD diagnosis. Written informed consent was obtained from all parents, and the children provided verbal assent to participate after sufficient explanation of the study was provided prior to enrollment. All study protocols were approved by the Institutional Review Board of SNUH (IRB No. 2008-116-1150).

Clinical evaluations

The children with ASD were assessed for autistic symptom severity according

to the Autism Diagnostic Observation Schedule (ADOS) (41) and Korean Childhood Autism Rating Scale, Second Edition (K-CARS-2) (42) at the Child and Adolescent Psychiatry Clinic in SNUH. In addition, social ability and competence were assessed using the Social Responsiveness Scale (SRS) (43) in children with ASD. The K-CARS-2 and SRS scores were also measured in the TD group. All participants were assessed for their intelligence using the Korean Educational Development Institute-Wechsler Intelligence Scale for Children-Revised (44) for school-age children with language and the Korean-Leiter International Performance Scale-Revised (45) for preschool and school-aged children without language. Among the various clinical symptom scales, we considered ADOS, which was assessed by experienced evaluators directly observing ASD children, as the main value. In addition, the Calibrated Severity Score (CSS) that corrected the differences between each ADOS version and module in the ADOS total score, was mainly considered.

Image acquisition and preprocessing

All participants were scanned using a Siemens Trio 3 T MRI scanner (Siemens Medical Systems, Erlangen, Germany) at SNUH. The whole MRI protocol took 35 min, and included structural MRI, diffusion tensor imaging (DTI), and rs-fMRI scans. The images of structural MRI were acquired with the following parameters: repetition time, 2100 ms; echo time, 3.71 ms; flip angle, 10°; voxel size, $1.0 \times 1.0 \times 1.0$ mm^3; field of view, 256 mm; slice number, 192 (sequential); slice thickness, 1.0 mm; and bandwidth, 200Hz/Px. The parameters of DTI were as follows: repetition time, 4000 ms; echo time, 88.0 ms; flip angle, 90°; voxel size, $1.9 \times 1.9 \times 2.0$ mm^3; field of view, 240 mm; slice number, 87 (interleaved); slice thickness, 2.0 mm; b-

value 1, 0 s/mm^2; b-value 2, 700 s /mm^2 and diffusion directions, 6. Finally, the parameters of fMRI were as follows: repetition time, 2000 ms; echo time, 30.0 ms; flip angle, 80°; voxel size, 3.0 × 3.0 × 3.0 mm^3; field of view, 220 mm; slice number, 48 (interleaved); matrix, 128 × 128 (or 64 × 64); and slice thickness, 3.0 mm. As the aim of this study is to explore the difference in brain functional connectivity between children with ASD and TD children and to identify the effects of OXTR variants on brain connectivity, we only analyzed fMRI images.

Some of the children needed to be sedated with oral chloral hydrate for immobility during the MRI scan. The medication was prescribed and administered carefully by certified psychiatrists at a safe dose for children (25–50 mg/kg; maximum dose, 1 g) after obtaining the parents' consent. Forty children with ASD and 15 TD children took the medication for sedation, and all TD children with medication were aged between 2 and 6 years.

rs-fMRI data were preprocessed using the DPARSF toolbox (46) together with the Statistical Parametric Mapping version 12 software (http://www.fil.ion.ucl.ac.uk/spm/) in the MATLAB environment. The first five time points in each dataset were discarded to allow for magnetization equilibrium. The remaining 185 volumes were analyzed. The preprocessing steps included the following: (a) slice timing correction was performed; (b) single-participant echo planar imaging (EPI) images were realigned using a six-parameter rigid body process to correct for head motion during data acquisition; (c) spatial normalization procedure transformed the realigned EPI images into a common stereotactic space by using an EPI template and resampling to 3-mm isotropic voxels; (d) spatial smoothing with a 6-mm full-width at half-maximum Gaussian kernel was performed;

and (e) linear detrend was performed. Six participants with a displacement of ≥ 3 mm between any two consecutive volumes were excluded. Therefore, 91 participants were finally included in the analysis, consisting of 41 children with ASD and 50 TD children.

Group independent component analysis (ICA)

After preprocessing, intrinsic networks were assessed using ICA and GIFT version 4.0 according to four major steps: (i) concatenation of all scans from 91 participants, (ii) data reduction, (iii) group ICA, and (iv) back reconstruction (47). Group ICA was performed using the infomax algorithm (48). The data were automatically decomposed into 25 components using the GIFT software. The statistical reliability of the independent component (IC) decomposition was tested using the Icasso toolbox (49). Visual inspection of the spatial patterns allowed us to remove components located in the cerebrospinal fluid or white matter or those that correlated poorly with gray matter, because they can be of an artifactual nature.

After removing all artifactual components, only the following 19 ICs survived for further analysis: the DMNs (IC9, IC12, IC18, IC22), cognitive control (CC) networks (IC13, IC16, IC17, IC21, IC23, IC25), auditory (AUD) network (IC7), SM networks (IC3, IC5, IC6, IC10), subcortical (SUB) network (IC15), and visual (VIS) networks (IC8, IC11, IC24).

For the selected set of ICs, we considered the following three outcome variables: (1) component spatial map, (2) between-component functional network connectivity (FNC), and (3) component power spectra. Component spatial maps were thresholded based on the distribution of voxel-wise t-statistics to identify voxels with strong and

consistent activation across participants to focus the analysis on the subset of voxels most representative of each network (50). From this point on, descriptions of component spatial maps refer to the thresholded maps containing the regions most relevant to the component time course (TC). FNC was estimated using Pearson's correlation coefficient between TC pairs (51). Participant-specific TCs were despiked based on the median absolute deviation implemented in 3dDespike3 and then filtered using a fifth-order Butterworth low-pass filter with a high-frequency cutoff of 0.08 Hz. Pairwise correlations were computed between TCs, resulting in a symmetric 19 × 19 correlation matrix for each participant. In all FNC analyses, correlations were converted to Z-scores using Fisher's transformation and then entered into statistical comparisons (50).

OXTR SNP genotyping

We collected whole blood samples from all subjects, and the samples were stored frozen. Genomic DNA extraction was performed using Axen™ Blood genomic DNA extraction kit (MG-P-01-100) and genotyping for single-nucleotide polymorphisms (SNP) of OXTR (rs2254298 and rs53576) was performed with the Taqman® SNP genotyping assays (Applied Biosystems). The quality of genomic DNA samples was assessed using a NanoDrop® ND-1000 UV-Vis Spectrophotometer, following which the genomic DNA was diluted to a concentration of 10 ng/$\mu\ell$ at 96 well PCR plates. The probes were labeled with FAM or VIC dye at the 5' end and a minor-groove binder and non-fluorescent quencher at the 3' end. Each primer and probe set was used in the Taqman genotyping assays (ID: C__15981334_10 for rs2254298 and C___3290335_20 for rs53576; Applied

Biosystems) from the information on the Applied Biosystems website (http://www.appliedbiosystems.com). SNP genotyping reactions were performed on QuantStudio™ Real-time polymerase chain reaction (PCR) system using the following cycles: 1 cycle at 50°C for 2 min; 1 cycle at 95°C for 10 min; 60 cycles at 95°C for 15 sec, then at 60°C for 1 min. The PCR was performed in a reaction mixture volume of TaqMan Genotyping Master Mix (2X) 2.5 µL, TaqMan assay (40x) 0.125 µL, DNA template (10 ng / µL) 2 µL, and nuclease-free water 0.375 µL. Once the PCR amplification is completed, the QuantStudio™ machines are used to perform allelic discrimination. During this process, the SDS v2.4 software measures the fluorescence and generates Rn values based on the signals from each well. Then the plates were analyzed and performed automatic or manual allele calls.

Quantitative DNA methylation with Pyrosequencing

Quantification of DNA methylation level at two CpG sites of OXTR was analyzed using Pyrosequencing. The DNA samples were subjected to bisulfite conversion to convert unmethylated cytosine residues to uracil, while leaving methylated cytosine residues intact. After bisulfite conversion, the PCR amplification was performed using primers specific to the region of interest. The primer sequences used for analysis were as follows: the forward sequence, OXTR-U-934_F (TTGAGTTTTGGATTTAGATAATTAAGGATT); the reverse sequence, OXTR-U-934_R (AATAAAATACCTCCCACTCCTTATTCCTA); and the sequencing primer, OXTR-U-934_seqF (AGAAGTTATTTTATAATTTTT). The PCR products were then purified and quantified using a gel electrophoresis. Pyrosequencing was performed using PyroMark Q48 Autoprep System (QIAGEN),

which uses sequencing-by-synthesis to detect the presence of methylated and unmethylated cytosine residues at single CpG sites. The pyrosequencing data was analyzed using PyroMark Q48 calculating the percentage of DNA methylation at each CpG site based on the ratio of the intensity of the signal from the methylated cytosine residues to the total signal from the methylated and unmethylated cytosine residues.

Statistical analyses

Spatial map voxels, FNC correlations, and spectral bins were compared between diagnostic groups (TD vs. ASD) using multiple regressions, with age, sex, and Full Scale IQ (FSIQ) score as covariates. The significant results were visualized using a plot that displays the log of the p-value with the sign of the corresponding t-statistic ($-$sign(t)log10(p)). This provides information on the direction and statistical power of the results.

We tested the interaction between SNP genetic variants and diagnosis on each imaging measures. Same as the above group comparison, genetic imaging analysis was performed on three imaging measures with same covariates. In the model, *y* represents the three measures, spatial map, FNC, and time course spectra, *β* refers estimated coefficients of the variables (diagnosis, genetic variants, and diagnosis × genetic variants), and *e* refers to an error. We investigated significant interaction effects between diagnosis and genetic variants to find out the impact of the OXTR genotype on brain functional connectivity in both groups.

$$y = \beta_0 + \beta_1 \times diagnosis + \beta_2 \times genetic\ variants + \beta_3 \times diagnosis \times genetic\ variants + e$$

Next, we also tested the interaction effect between diagnosis and the methylation level of two CpG sites of OXTR to find out whether there were differences in the resting functional connectivity between groups according to the methylation level of the OXTR. Each variable denotes the same as above.

$$y = \beta_0 + \beta_1 \times diagnosis + \beta_2 \times methylation\ level + \beta_3 \times diagnosis \times methylation\ level + e$$

All tests were adjusted for multiple comparisons using the false discovery rate (FDR) method at a significance level of 0.05.

Finally, correlation analyses between significant outcome measurements and ASD symptom scores were performed using Pearson analyses. The neuroimaging data and clinical ASD features were adjusted for age, sex, and FSIQ score using multiple linear regression models to remove the effects of covariates. Specifically, a correlation analysis was performed using the statsmodels.api.OLS package (https://www.statsmodels.org/dev/generated/statsmodels.regression.linear_model.OLS.html).

Results

Participant characteristics (Table 1)

Demographic and clinical characteristics of the ASD and TD groups are presented in Table 1. The mean age of ASD group was significantly lower than that of TD group (4.46 ± 1.91 and 6.94 ± 2.73 for the ASD and TD groups, respectively), and there was significant difference in sex composition (32 boys and 9 girls in the ASD group and 23 boys and 27 girls in the TD group) between the two groups. The CARS and SRS scores were significantly higher in the ASD group than in the TD group because these scales measured the symptom severity of ASD. The FSIQ score was significantly lower in the ASD group than in the TD group; therefore, we included age, sex, and the FSIQ score as covariates.

The genotyping results of two SNPs are shown in Table 1 and Table 2. There were no significant differences in genotyping results between the two groups. For the genetic analyses of rs2254298, since the homozygous recessive genotype (AA) was rare in both group, the genotype variant was divided into two groups: the AA + AG (A carriers) group and the GG group. Similarly, the genotypes of the rs53576 was divided into two groups (the AA group and the AG + GG group) due to the rare number of the subjects with the homozygous dominant genotype (GG).

The results of epigenetic analysis are also shown in Table 1. When comparing the methylation levels of the two CpG sites in the ASD and TD groups, there was a significant difference between the two groups in CpG_924 (pos 1), and ASD children showed more increased methylation level than TD children (58.03 ± 6.71 for the

ASD group and 51.97 ± 4.05 for the TD group, $p < .000$). However, there was

no significant difference in the methylation level of CpG_934 (pos 2).

Table 1. Demographic and clinical characteristics

Variables		Groups ASD (n = 41)			TD (n = 50)			P -value
		Mean	SD	n	Mean	SD	n	
Age (years)		4.46	1.91	41	6.94	2.73	50	0.009
Sex	Boy			32			23	0.002
	Girl			9			27	
Sedation				40			15	
ADOS score								
	Communication	5.54	1.83	39	-	-	-	
	Social interaction	10.38	2.37	39	-	-	-	
	Behavior	1.82	1.34	39	-	-	-	
	Total	17.77	3.96	39	-	-	-	
	CSS	7.39	1.64	38	-	-	-	
FSIQ score		55.61	18.44	38	111.1	15.5	49	< .000
CARS score		30.76	5.06	40	15.38	0.63	45	< .000
SRS score								
	Awareness	12.54	4.14	28	5.03	2.74	30	< .000
	Cognition	19.79	5.43	28	5.83	3.32	30	< .000

		Mean	SD	N	Mean	SD	N	p
	Communication	33.54	11.13	28	6.43	3.67	30	< .000
	Motivation	14.5	5.44	28	4.47	3.3	30	< .000
	Responsiveness	13.96	7.93	28	2.5	2.84	30	< .000
	SCI	80.36	22.96	28	21.77	10.38	30	< .000
	Total	94.32	29.88	28	24.27	11.54	30	< .000
rs2254298	AA, AG			20			24	0.941
	GG			21			26	
rs53576	AA			15			21	0.599
	GG, AG			26			29	
Methylation level (%)	CpG_924 (pos1)	58.03	6.71	40	51.97	4.05	40	< .000
	CpG_934 (pos2)	44.64	5.08	40	43.11	5.03	40	0.179

Abbreviations: ADOS, Autism Diagnostic Observation Schedule; ASD group, children with autism spectrum disorder; CARS, Childhood Autism Rating Scale; CSS, Calibrated Severity Score; FSIQ, Full Scale IQ; SCI, Social Communication and Interaction; SD, standard deviation; SRS, Social Responsiveness Scale; TD group, children with typical development

Table 2. Genotypic distributions of the OXTR Genes in ASD and TD Groups.

Variables		Groups		P - value
		ASD (n = 41)	TD (n = 50)	
rs2254298	Genotype (%)			0.956
	AA	4 (9.8)	6 (12)	
	AG	16 (39.0)	18 (36)	
	GG	21 (51.2)	26 (52)	
rs53576	Genotype (%)			0.186
	AA	15 (36.6)	21 (42.0)	
	AG	16 (39.0)	24 (48.0)	
	GG	10 (24.4)	5 (10.0)	

Abbreviations: ASD, autism spectrum disorder; TD, children with typical development

Group differences of intrinsic network based on ICA

After visual inspection of the spatial maps, we selected 19 of the 25 ICs generated from the ICA group, including DMN and CC, AUD, SM, SUB, and VIS networks (Figure 1). In the following, we summarize each set of results, starting with the spatial map, followed by the FNC, and then the spectra.

In total, 13 out of the 19 ICs represented spatial map group differences using an FDR-corrected threshold of $p < 0.05$. The results are summarized in Figure 2. The ICs representing group differences could be grouped into four intrinsic networks: the DMN and CC, SUB, and VIS networks. The CC network included six networks (components [C] 13, C16, C17, C21, C23, and C25), the DMN contained four networks (C9, C12, C18, and C22), the SUB network contained one network (C15), and the VIS network contained two networks (C8 and C11). The composite views demonstrating group differences are shown in Figure 2. Compared with TD children, children with ASD had lower measures in the CC network and DMN. Stronger measures in the SUB and VIS networks were found in children with ASD than in TD children. A complete list of these regions is provided in Table 3.
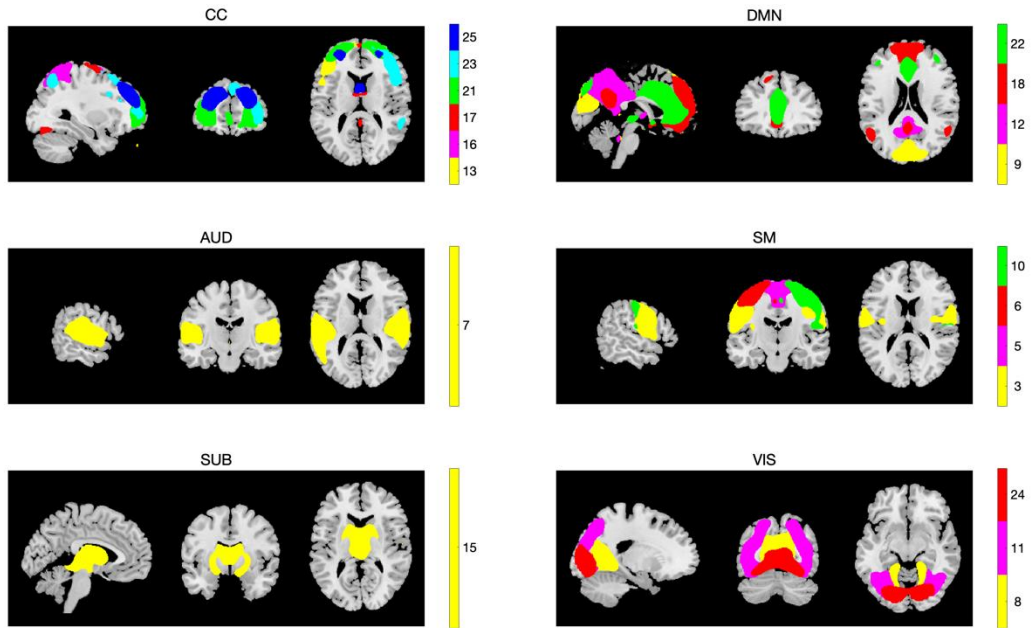
Figure 1. Independent components (ICs) generated from visual inspection of spatial maps

All the selected ICs (n = 19) were arranged using intrinsic networks. The component spatial maps are shown in color (t ≥ 1).

*Abbreviations: IC, independent component; CC, cognitive control; DMN, default mode network; AUD, auditory; SM, somatomotor; SUB, subcortical; VIS, visual
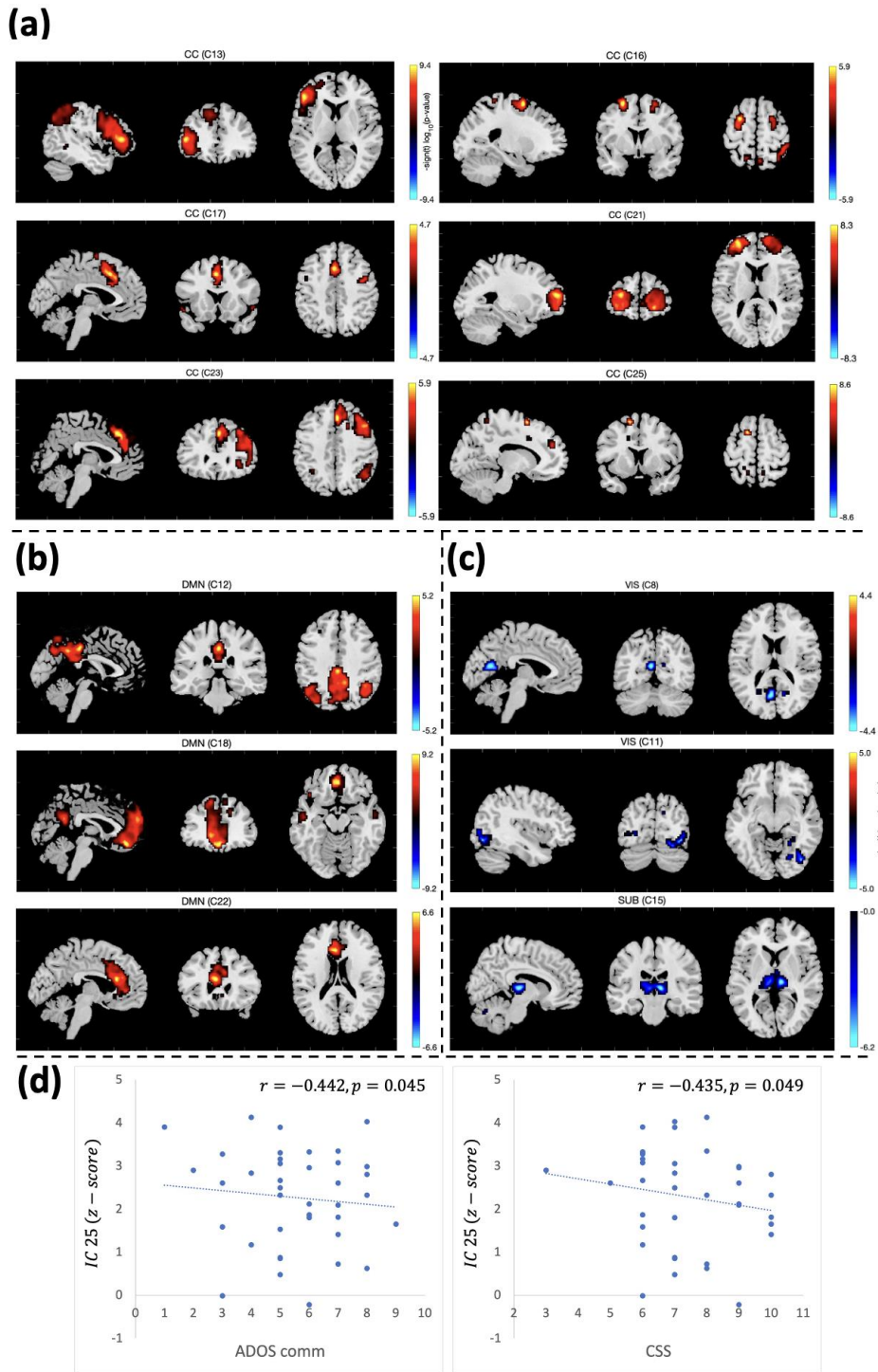
Figure 2. Independent components (ICs) with significant differences between groups using spatial maps

(a) Significant results of the CC network revealing between-group effects of diagnosis (areas colored with blue means ASD < TD) (p < 0.05 corrected for multiple comparisons using FDR). (b) Significant results of the DMN revealing between-group effects of diagnosis (areas colored with blue means ASD < TD) (p < 0.05 corrected for multiple comparisons using FDR). (c) Significant results of the VIS and SUB networks revealing between-group effects of diagnosis (areas colored with red means ASD > TD) (p < 0.05 corrected for multiple comparisons using FDR). (d) Significant correlation results between IC 25 spatial map Z-score and clinical scores (ADOS scores and CSSs) in ASD.

*Abbreviations: CC, cognitive control; FDR, false discovery rate; DMN, default mode network; SUB, subcortical; VIS, visual; IC, independent component; ADOS, Autism Diagnostic Observation Schedule; CSS, Calibrated Severity Score; comm, communication).

Table 3. Regions showing significant resting state (RS) functional connectivity (FC) differences between children with ASD and TD in the intrinsic networks (*Age-, FSIQ-, sex-adjusted linear model (p<0.05, clusterwise FWE-corrected for multiple comparisons)

IC number	cluster	Region	t values*	Cluster extent (no. of voxels)	MNI coordinates (X, Y, Z)
CC (Decreased RS FC in ASD)					
IC13	cluster1	Left inferior frontal cortex	-7.27	1174	-48, 36, 6
	cluster2	Left superior parietal cortex	-5.37	346	-42, -51, 57
	cluster3	Left middle frontal cortex	-4.76	155	-30, 9, 54
	cluster4	Left superior frontal cortex	-4.11	106	0, 27, 45
IC16	cluster1	Left superior frontal cortex	-5.37	87	-24, 3, 63
	cluster2	Left supramarginal cortex	-4.93	160	-63, -33, 33
	cluster3	Right supramarginal cortex, Right superior parietal cortex	-4.62	102	42, -42, 48
IC17	cluster1	Left superior frontal cortex	-4.52	94	-3, 18, 45
IC21	cluster1	Left middle frontal cortex	-6.66	586	-27, 54, 12
	cluster2	Right anterior orbital cortex, Right superior frontal cortex	-6.32	537	24, 54, -6
IC23	cluster1	Right superior frontal cortex	-5.27	317	3, 30, 42
	cluster2	Right middle frontal cortex	-5.26	430	54, 21, 39
			-5.15	194	33, 45, 6
	cluster3	Right angular cortex	-4.07	59	51, -48, 27
IC25	cluster1	Left superior frontal cortex	-6.81	35	-12, 9, 63
DMN (Decreased RS FC in ASD)					
IC12	cluster1	Bilateral posterior cingulate cortex	-4.9	343	0, -30, 39
	cluster2	Left angular cortex	-4.12	57	-42, -63, 45
	cluster3	Right angular cortex	-4.12	102	42, -51, 39

IC18	cluster1	Right medial frontal cortex	-6.94	1905	3, 42, -18
	cluster2	Bilateral precuneus	-6.27	149	0, -54, 24
	cluster3	Left orbital part of the inferior frontal cortex	-4.95	60	-36, 30, -9
IC22	cluster1	Bilateral anterior cingulate cortex	-5.81	621	-3, 27, 18
	cluster2	Left middle frontal cortex	-5.17	72	-33, 39, 24
VIS (Increased RS FC in ASD)					
IC8	cluster1	Left precuneus, cuneus	4.38	106	-3, -66, 15
IC11	cluster1	Right inferior occipital cortex	5.22	119	42, -78, -12
SUB (Increased RS FC in ASD)					
IC15	cluster1	Right thalamus proper	5.38	177	9, -21, 6

Abbreviations: FWE, family-wise error; IC, independent component; MNI, Montreal Neurological Institute; CC, cognitive control; DMN, default mode network; VIS, visual; SUB, subcortical; rs FC, resting-state functional connectivity

The FNC results are shown in Figure 3. All significant FNCs between the ICs and intrinsic network-averaged FNC differences are shown. In general, TD children demonstrated more positive correlations among ICA TCs across networks than did children with ASD (more orange/red in the figure), whereas the FNC between the SM, VIS, and SUB networks was over-connected in children with ASD compared with TD children (more blue in the figure). The CC network played a major role in comparisons between diagnostic groups. Eight of the same networks showing differences in the spatial map (CC network [C13, C16, C17, C23, C25], DMN [C9, C22], SUB network [C15], and VIS network [C11]) also demonstrated FNC differences between the ASD and TD groups.

Finally, diagnostic group differences in spectral power were evaluated. Figure 4 shows a spectral image of the components (y-axis) by spectra (x-axis), with significant differences marked in orange (TD > ASD) or blue (TD < ASD). From this, it is clear that the TD group had greater power in low-frequency bands than the ASD group, and the ASD group had more power in high-frequency bands than the TD group. The general trends of all component spectra tended to be similar, with some having slightly stronger effects that passed significance.
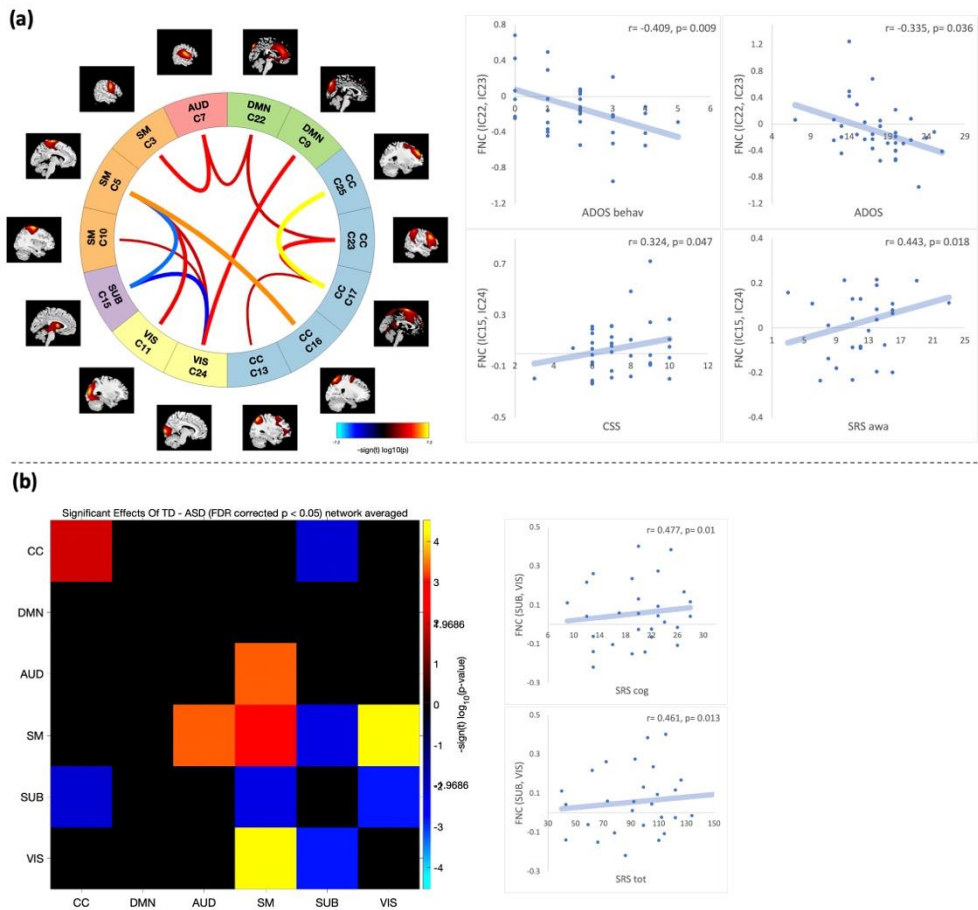
Figure 3. Resting-state FNC differences between two groups

(a) Resting-state FNC differences between children with ASD and TD children. A diagram shows intrinsic networks with a significantly different pair-wise connectivity between diagnostic groups. The red lines indicate stronger connectivity in TD children compared with children with ASD, and the blue line indicates weaker connectivity in TD children compared with children with ASD. Significant correlation results (between FNC and clinical scores [ADOS, SRS, CSS]) are also plotted. (b) Intrinsic network-averaged FNC differences between diagnostic groups. Significant correlation results (between FNC network averaged and clinical scores [SRS]) are also plotted.

*Abbreviations: FNC, functional connectivity; ADOS, Autism Diagnostic

Observation Schedule; SRS, Social Responsiveness Scale; CSS, Calibrated Severity Score; behav, behavior; awa, awareness; cog, cognition; tot, total; CC, cognitive control; DMN, default mode network; SUB, subcortical; VIS, visual; SM, somatomotor; AUD, auditory; IC, independent component; FDR, false discovery rate
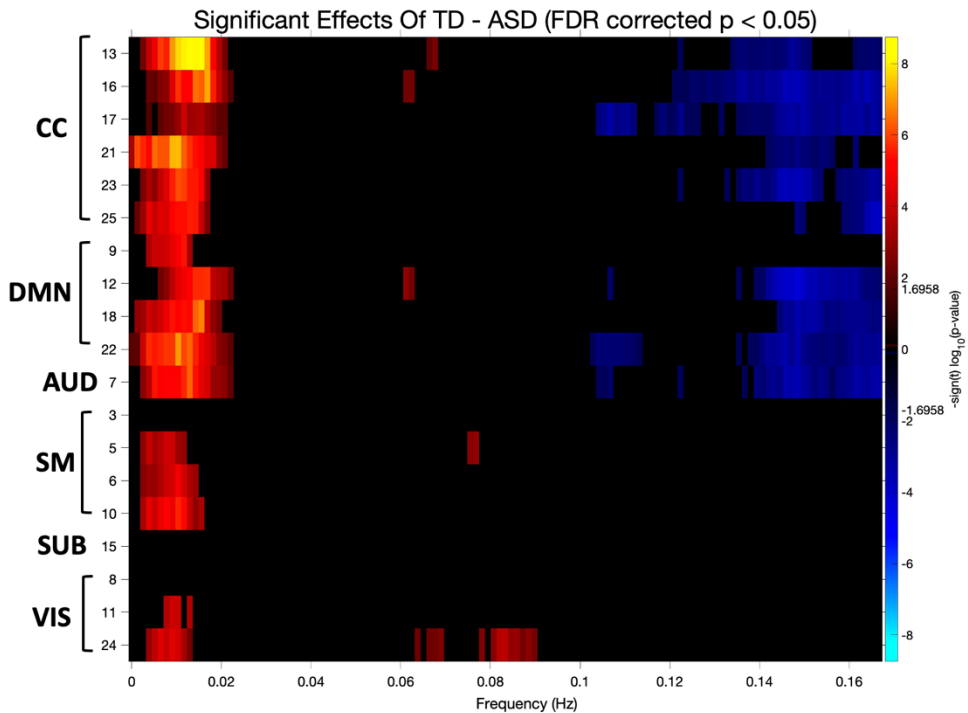
Figure 4. Between-group differences with spectra

Significant differences in spectral power (thresholded at $p < 0.05$, corrected for multiple comparisons) for TD – ASD contrasts. Color maps in panels show the power differences at each frequency over each component separately.

*Abbreviations: FDR, false discovery rate; CC, cognitive control; DMN, default mode network; AUD, auditory; SM, somatomotor; SUB, subcortical; VIS, visual

Correlation between the aberrant intrinsic networks and clinical scores

In children with ASD, significant correlations were found between rs FC abnormalities and clinical scores (Table 4, Figure 2, and Figure 3). In the spatial map, the FC in the ASD group was significantly correlated with the ADOS sub-score for communication (r = –0.442, p = 0.045) and CSS (r = –0.435, p = 0.049) (Figure 2). In the FNC, under-connectivities of the CC network, DMN, and SM network were negatively correlated with several sub-scores of the SRS and ADOS in children with ASD. In contrast, the over-connectivity between the SUB and VIS networks showed positive correlations with SRS sub-scores and CSS (Figure 3). The full results of the clinical correlation analysis are shown in the Table 5.

Table 4. Significant results of correlation analyses in children with ASD

Outcome measurements		Clinical correlation	
		Pearson corr (r)	Sig (p)
Spatial map			
IC25	ADOS_com	-0.442	0.045
	CSS	-0.435	0.049
FNC			
IC5, IC16	SRS_com	-0.428	0.022
	SCI	-0.396	0.036
	SRS_tot	-0.383	0.043
IC5, IC11	ADOS_socint	-0.332	0.038
IC22, IC23	ADOS_behav	-0.409	0.009
	ADOS	-0.335	0.036
IC5, IC24	SRS_res	-0.377	0.047
	SRS_tot	-0.372	0.051
IC13, IC17	SRS_awa	-0.442	0.018
	SRS_com	-0.474	0.010
	SCI	-0.430	0.022
	SRS_tot	-0.417	0.027
IC15, IC24	CSS	0.324	0.047
	SRS_awa	0.443	0.018
FNC (network averaged)			
SUB, VIS	SRS_cog	0.477	0.01
	SRS_com	0.373	0.05
	SRS_mot	0.393	0.038
	SRS_res	0.400	0.034
	SCI	0.461	0.013
	SRS_tot	0.461	0.013

Abbreviations: IC, independent component; ADOS, Autism Diagnostic Observation Schedule; SRS, Social Responsiveness Scale; com; communication; awa, social awareness; SCI, Social Communications Index; CSS, Calibrated Severity Score; behave, restricted and repetitive behaviors; cog, social cognition; mot, social motivation; res, restricted interests and repetitive behaviors; SUB, subcortical; VIS, visual

Table 5. Results of correlation analyses on FNC in children with ASD

		ADOS_com	ADOS_soc	ADOS_beh	ADOS_tot	ADOS_css	CARS	SRS_awa	SRS_cog	SRS_com	SRS_mot	SRS_res	SRS_sci	SRS_tot
IC17, IC25	Pearson corr (r)	-0.216	-0.077	-0.005	-0.141	-0.241	0.178	0.003	0.147	0.133	0.012	0.012	0.106	0.083
	Sig (p)	0.186	0.638	0.973	0.39	0.144	0.269	0.986	0.453	0.498	0.947	0.947	0.588	0.672
IC5, IC16	Pearson corr (r)	-0.011	-0.087	-0.299	-0.163	-0.05	-0.135	-0.313	-0.349	-0.428	-0.151	-0.3	-0.396	-0.383
	Sig (p)	0.943	0.595	0.064	0.318	0.764	0.405	0.103	0.068	0.022	0.441	0.119	0.036	0.043
IC17, IC23	Pearson corr (r)	-0.123	0.005	-0.026	-0.058	0.049	0.18	-0.1	0.119	0.094	0.197	0.052	0.102	0.091
	Sig (p)	0.454	0.973	0.871	0.722	0.766	0.265	0.61	0.544	0.63	0.313	0.791	0.602	0.641
IC3, IC7	Pearson corr (r)	0.216	0.167	0.094	0.236	0.264	0.383	-0.276	-0.006	-0.15	0.16	-0.131	-0.094	-0.108
	Sig (p)	0.186	0.308	0.568	0.146	0.108	0.014	0.153	0.971	0.445	0.415	0.503	0.633	0.582
IC9, IC24	Pearson corr (r)	0.222	-0.001	0.121	0.139	0.048	0.295	0.102	0.146	0.211	0.201	0.046	0.207	0.168
	Sig (p)	0.173	0.994	0.459	0.397	0.774	0.064	0.604	0.457	0.28	0.304	0.812	0.288	0.39
IC5, IC11	Pearson corr (r)	0.242	-0.332	0.007	-0.081	-0.029	0.147	-0.282	0.054	-0.14	-0.139	-0.157	-0.144	-0.153
	Sig (p)	0.136	0.038	0.962	0.619	0.862	0.362	0.144	0.781	0.474	0.477	0.424	0.464	0.436
IC7, IC22	Pearson corr (r)	0.207	0.175	-0.186	0.133	0.243	0.338	0.094	0.114	0.135	0.163	0.041	0.152	0.125
	Sig (p)	0.203	0.284	0.255	0.419	0.141	0.032	0.631	0.562	0.491	0.404	0.834	0.439	0.523
IC22, IC23	Pearson corr (r)	-0.014	-0.287	-0.409	-0.335	-0.237	-0.285	-0.106	0.117	-0.057	-0.103	-0.049	-0.044	-0.047

	Sig (p)	0.932	0.075	0.009	0.036	0.15	0.074	0.59	0.55	0.77	0.598	0.804	0.822	0.811
IC5, IC24	Pearson corr (r)	0.064	0.035	-0.201	-0.017	0.09	-0.261	0.221	-0.32	-0.365	-0.201	-0.377	-0.351	-0.372
	Sig (p)	0.695	0.828	0.219	0.916	0.589	0.103	0.256	0.096	0.055	0.303	0.047	0.066	0.051
IC10, IC24	Pearson corr (r)	-0.01	0.057	-0.143	-0.028	0.033	-0.152	0.288	-0.079	0.024	0.044	-0.119	0.058	0.009
	Sig (p)	0.949	0.727	0.381	0.865	0.843	0.347	0.136	0.686	0.903	0.82	0.546	0.766	0.961
IC13, IC17	Pearson corr (r)	-0.02	-0.207	-0.012	-0.124	-0.034	0.144	-0.442	-0.218	-0.474	-0.229	-0.33	-0.43	-0.417
	Sig (p)	0.901	0.205	0.939	0.449	0.835	0.374	0.018	0.264	0.01	0.239	0.085	0.022	0.027
IC5, IC15	Pearson corr (r)	-0.028	0.087	0.051	0.074	0.072	0.107	-0.096	-0.144	-0.071	-0.026	-0.103	-0.096	-0.102
	Sig (p)	0.862	0.598	0.753	0.652	0.666	0.508	0.626	0.462	0.716	0.892	0.6	0.624	0.605
IC15, IC24	Pearson corr (r)	0.097	0.184	0.164	0.219	0.324	0.205	0.443	0.323	0.324	0.117	0.173	0.355	0.315
	Sig (p)	0.553	0.261	0.316	0.179	0.047	0.203	0.018	0.093	0.092	0.55	0.378	0.063	0.101
SM_VIS	Pearson corr (r)	0.164	-0.049	0.077	0.075	0.259	0.399	-0.02	0.062	-0.121	0.152	-0.092	-0.014	-0.037
	Sig (p)	0.317	0.762	0.64	0.647	0.115	0.01	0.915	0.75	0.537	0.439	0.639	0.941	0.849
AUD_SM	Pearson corr (r)	0.003	-0.035	0.026	-0.001	0.036	0.365	-0.254	-0.03	-0.171	0.122	-0.065	-0.114	-0.104
	Sig (p)	0.984	0.83	0.874	0.991	0.83	0.02	0.191	0.878	0.383	0.535	0.742	0.56	0.596
SM_SM	Pearson corr (r)	-0.027	0.096	-0.078	0.019	0.115	0.105	0.223	0.293	0.166	0.238	0.062	0.254	0.207
	Sig (p)	0.867	0.557	0.636	0.907	0.488	0.518	0.252	0.13	0.396	0.222	0.753	0.192	0.288

CC_CC	Pearson corr (r)	0.146	0.071	-0.112	0.075	0.209	0.409	0.093	0.204	0.127	0.39	0.184	0.222	0.219
	Sig (p)	0.372	0.665	0.496	0.648	0.206	0.008	0.635	0.296	0.518	0.039	0.346	0.255	0.261
SUB_VIS	Pearson corr (r)	0.158	0.084	0.059	0.142	0.218	0.117	0.342	0.477	0.373	0.393	0.4	0.461	0.461
	Sig (p)	0.334	0.61	0.72	0.387	0.187	0.47	0.074	0.01	0.05	0.038	0.034	0.013	0.013
SUB_SM	Pearson corr (r)	-0.059	0.043	0.104	0.045	-0.001	0.158	0.119	0.042	0.08	0.122	0.047	0.101	0.089
	Sig (p)	0.719	0.79	0.525	0.785	0.997	0.328	0.543	0.831	0.685	0.534	0.812	0.605	0.649
SUB_CC	Pearson corr (r)	-0.344	-0.09	-0.081	-0.231	-0.378	-0.13	-0.203	-0.219	-0.099	-0.118	-0.031	-0.17	-0.136
	Sig (p)	0.031	0.583	0.62	0.157	0.019	0.422	0.298	0.262	0.616	0.547	0.871	0.385	0.487

Effects of the genetic risk of OXTR on resting-state functional connectivity

We summarized the results of the imaging genetic analysis of the two SNPs (rs2254298 and rs53576) in the order of FNC, spatial map, and time course spectra. For rs2254298, a total of 8 pairs of ICs (3 CC-CCs [C25-C17, C13-C17, and C23-C17], 1 DMN-DMN [C12-C18], 1 CC-SM [C16-C5], 1 CC-VIS [C16-C11], and 2 VIS-SMs [C11-C10 and C11-C5]) showed significant differences between the two groups according to the presence of the risk allele (A) (Figure 5). In the ASD group, decreased FCs were observed in the case of having at least one A allele in all 8 FNCs, whereas A carriers showed increased FCs in the TD group, which showed significant differences between the two groups.

The FNC results with significant interaction effects of rs53576 and diagnosis are shown in Figure 6 and 7. Most IC pairs presented similar results with the rs2254298 analyses above. In a total of 10 FNCs (2 CC-CCs [C17-C25 and C16-C17], 2 DMN-CCs [C22-C23 and C22-C25], 3 CC-SMs [C16-C5, C16-C6, and C21-C6], 1 DMN-AUD [C22-C7], 1 DMN-VIS [C24-C9], and 1 SM-VIS [C5-C24]), the A carriers in the TD group showed increased connectivities, while most of those in the ASD group showed decreases or less increases in connectivity (Figure 6). However, one FNC (SUB-SM [C15-C5]) showed a significant result in the opposite direction to the results above, and the FC increased in A carriers of ASD group and reduced in subjects with A allele among TD group. In addition, there were significant differences in the network-averaged FNCs with interaction effects of rs53576 and diagnosis (Figure 7). Similarly, two FNCs including SUB network (SUB-SM and SUB-VIS) showed increased FCs in A carriers with ASD and decreased FCs in those

with TD. In the other two FNCs not including SUB network (CC-SM and VIS-SM), lower connectivities were observed in the ASD group than the TD group, the same as the overall trend.
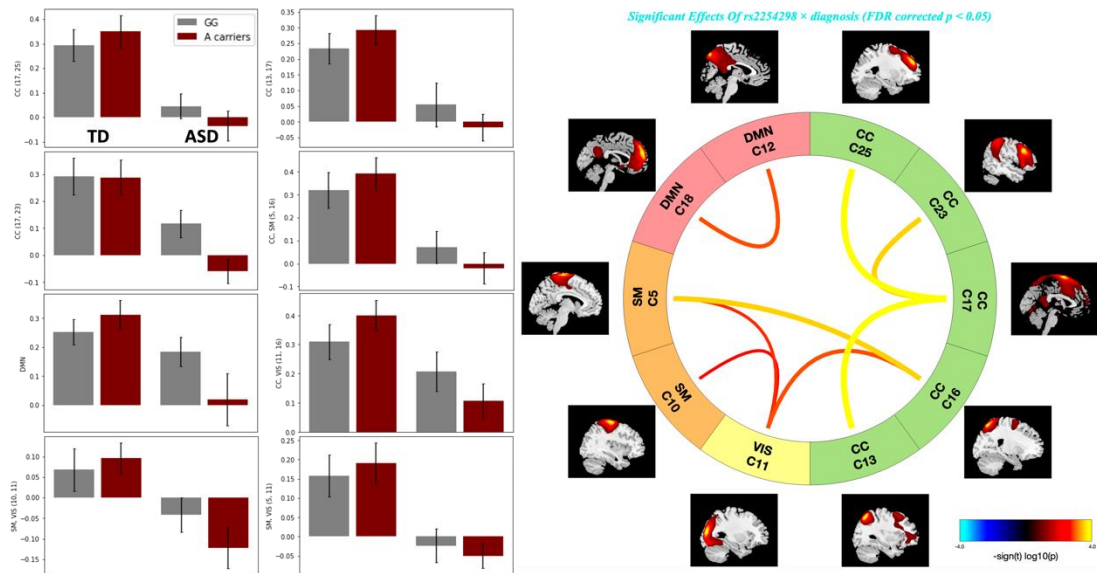
Figure 5. Significant effects of interaction between diagnosis and rs2254298 of OXTR with FNC

Children with ASD showed significantly decreased intrinsic connectivities compared to TD children associated with the risk allele of rs2254298 in 8 FNCs: 3 CC-CCs (C25-C17, C13-C17, and C23-C17), 1 DMN-DMN (C12-C18), 1 CC-SM (C16-C5), 1 CC-VIS (C16-C5), and 2 VIS-SMs (C11-C10 and C11-C5). ($p < 0.05$ corrected for multiple comparisons using FDR)

3 7
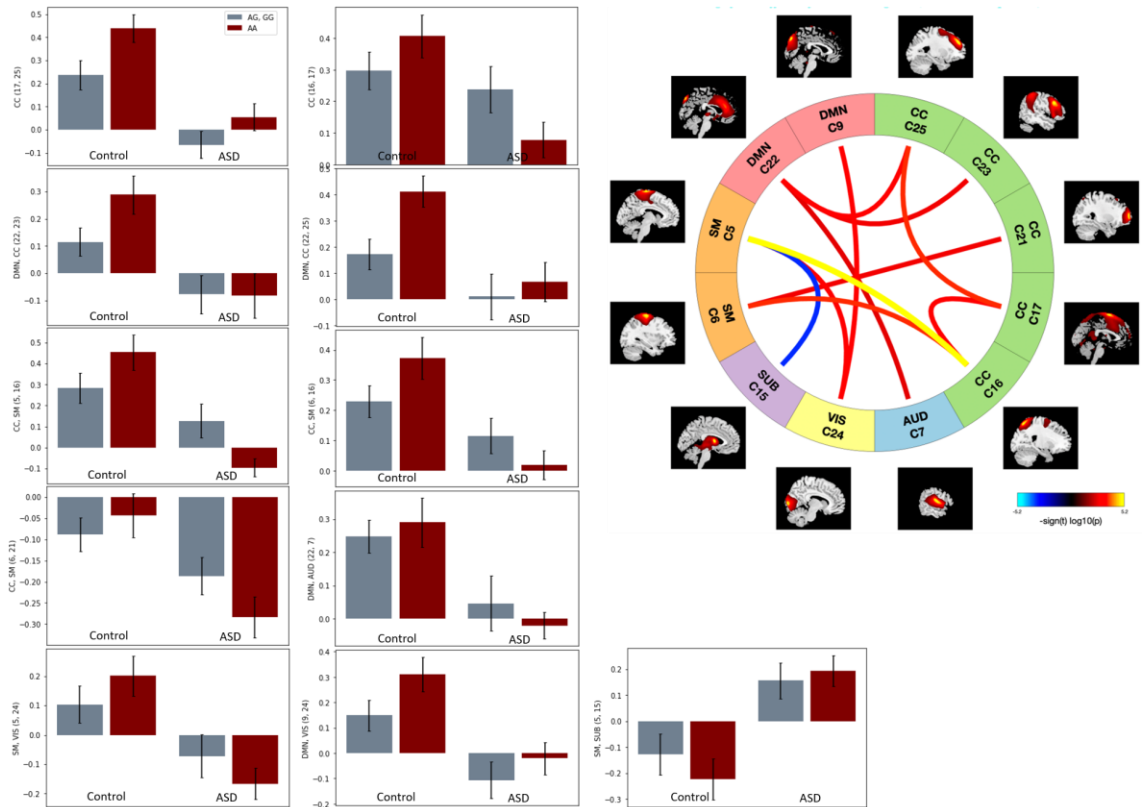
Figure 6. Significant effects of interaction between diagnosis and rs53576 of OXTR with FNC

Children with ASD showed significantly decreased intrinsic connectivities compared to TD children associated with the risk allele of rs53576 in 10 FNCs: 2 CC-CCs (C17-C25 and C16-C17), 2 DMN-CCs (C22-C23 and C22-C25), 3 CC-SMs (C16-C5, C16-C6, and C21-C6), 1 DMN-AUD (C22-C7), 1 DMN-VIS (C24-C9), and 1 SM-VIS (C5-C24). There was only 1 FNC (SUB-SM [C15-C5]),which showed increased functional connectivity in A carriers of ASD group and reduced connectivity in subjects with A allele in TD group. ($p < 0.05$ corrected for multiple comparisons using FDR)
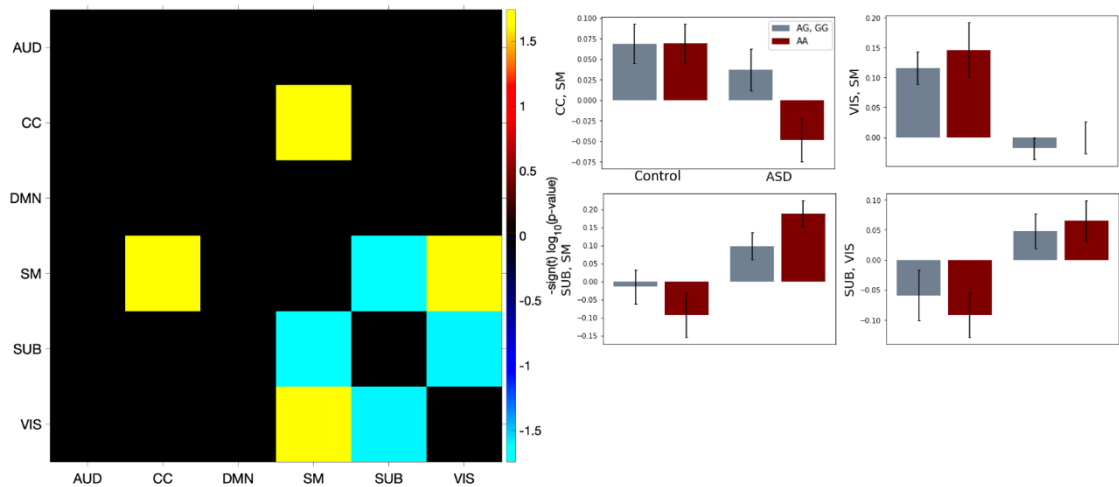
Figure 7. Significant effects of interaction between diagnosis and rs53576 of OXTR with FNC (network-wise analyses)

A allele carriers in ASD group showed significantly increased FNCs including SUB network (SUB-VIS and SUB-SM). FNCs including CC, SM and VIS networks decreased in A carriers among ASD group.

In spatial map analysis, we observed significant effect of the interaction between diagnosis and risk allele of rs2254298 on resting FCs of 4 ICs: 3 ICs of CC network (C13, C21, and C25) and 1 IC of DMN (C18) (Table 6 and Figure 8). For rs53576, 5 ICs showed significant effect of the interaction between diagnosis and genotype: 4 ICs of CC network (C25, C21, C16 and C13) and 1 IC of DMN (C18) (Table 7 and Figure 9). Both of rs2254298 and rs53576 showed similar results with spatial map analyses. In the TD group, FCs increased in A allele carriers, but in the ASD group, connectivities increased significantly less than the TD children or decreased associated with A allele.

We evaluated whether there were significant differences in spectral power according to the genotype of rs2254298 and rs53576 in the two groups. Similar to the between group analyses, in 8 ICs (4 DMNs [C9, C12, C18, and C22], 2 CCs [C13 and C16], 1 AUD [C7], and 1 SM [C3]) for rs2254298 and 5 ICs (1 DMN [C12], 1 CC [C13], 1 AUD [C7], and 2 VISs [C8 and C24]) for rs532576, A allele carriers in TD group showed increased spectral power in low-frequency bands than those in the ASD group (Figure 10). However, we did not observe any component with higher spectral power in high-frequency bands.

Table 6. Regions showing significant differences of FC associated with OXTR rs2254298 genotype between children with ASD and TD

IC number	cluster	Region	t values*	Cluster extent (no. of voxels)	MNI coordinates (X, Y, Z)
CC (Decreased RS FC)					
IC13	cluster1	Left triangular part of the inferior frontal cortex, Left middle frontal cortex, Left orbital part of the inferior frontal cortex	5.972	1009	-44, 37, 6
	cluster2	Left middle frontal cortex	3.495	287	-40, 22, 32
	cluster3	Left opercular part of the inferior frontal cortex, Left precentral cortex, Left middle frontal cortex	3.583	138	-54, 15, 30
IC21	cluster1	Left middle frontal cortex, Left triangular part of the inferior frontal cortex, Left lateral orbital cortex, Left superior frontal cortex	5.549	414	-39, 49, -2
	cluster2	Right anterior orbital cortex, Right superior frontal cortex, Right middle frontal cortex	4.485	243	24, 54, -6
IC25	cluster1	Left middle frontal cortex, Left superior frontal cortex	3.236	132	-15, 48, 30
	cluster2	Left superior frontal cortex, Left middle frontal cortex	4.034	31	-23, 30, 45
DMN (Decreased RS FC)					
IC18	cluster1	Bilateral superior frontal cortex, Bilateral middle frontal cortex, Bilateral medial frontal cortex, Left anterior cingulate cortex	4.776	1314	-6, 51, 33

*Age-, FSIQ-, sex-adjusted linear model (p<0.05, clusterwise FWE-corrected for multiple comparisons)

Table 7. Regions showing significant differences of FC associated with OXTR rs53576 genotype between children with ASD and TD

IC number	cluster	Region	t values*	Cluster extent (no. of voxels)	MNI coordinates (X, Y, Z)
CC (Decreased RS FC)					
IC13	cluster1	Left triangular part of the inferior frontal cortex, Left middle frontal cortex, Left orbital part of the inferior frontal cortex	7.132	776	-45, 36, 6
	cluster2	Left opercular part of the inferior frontal cortex, Left middle frontal cortex	4.749	106	-38, 20, 30
	cluster3	Left superior parietal lobule	4.434	97	-41, -51, 60
IC16	cluster1	Left superior frontal cortex, Left middle frontal cortex	7.001	25	-24, 3, 63
IC21	cluster1	Left middle frontal cortex, Left superior frontal cortex, Left triangular part of the inferior frontal cortex, Left anterior orbital cortex	4.259	235	-24, 51, -3
	cluster2	Left middle frontal cortex, Left superior frontal cortex	3.259	58	-30, 60, 12
	cluster3	Right anterior orbital cortex, Right superior frontal cortex, Right lateral orbital cortex	4.579	30	24, 54, -9
IC25	cluster1	Left superior frontal cortex, Left middle frontal cortex	3.797	12	-12, 9, 63
DMN (Decreased RS FC)					
IC18	cluster1	Bilateral superior frontal cortex medial segment, Left superior frontal cortex, Left frontal pole, Left anterior cingulate cortex	5.519	680	-6, 57, 18
	cluster2	Left medial frontal cortex, Left superior frontal cortex medial segment, Left superior frontal cortex	3.291	63	-12, 48, -12

*Age-, FSIQ-, sex-adjusted linear model (p<0.05, clusterwise FWE-corrected for multiple comparisons)
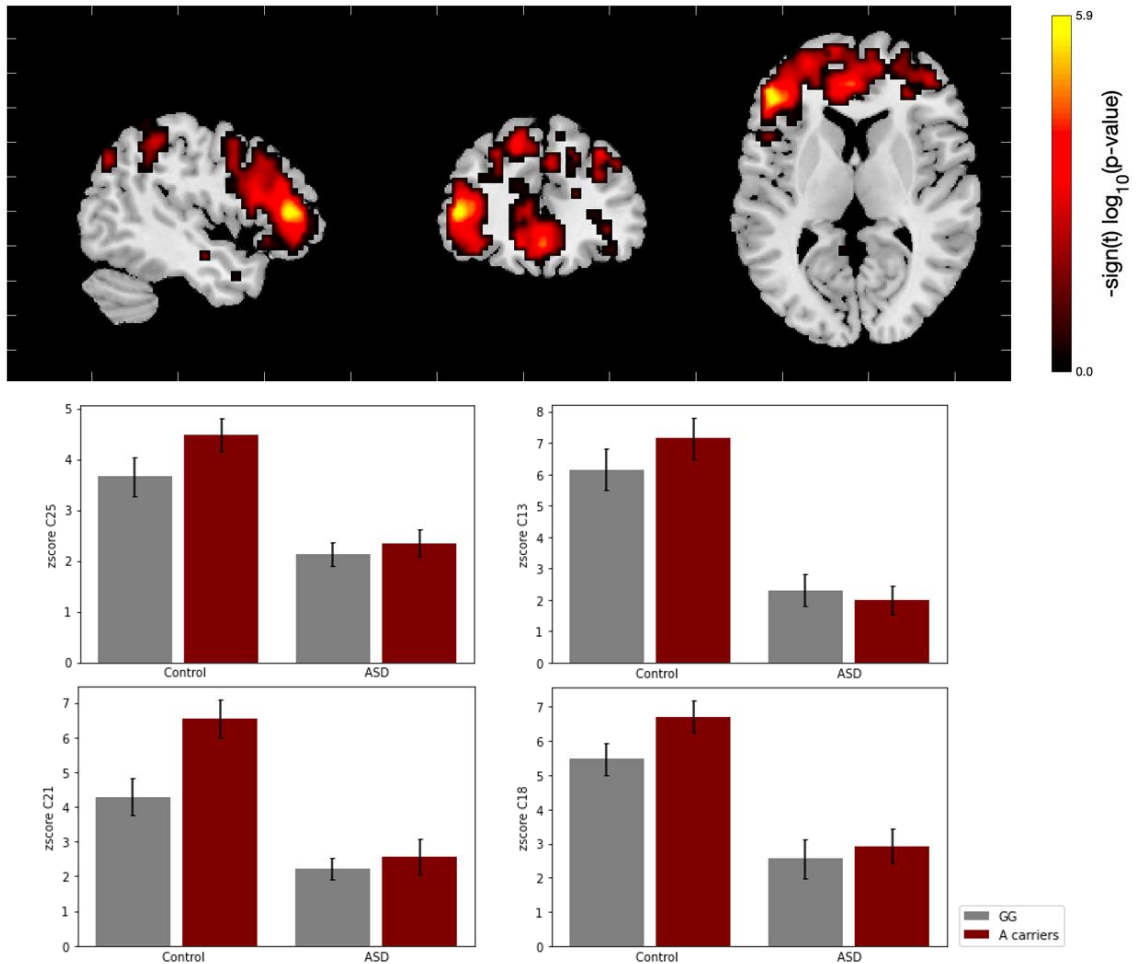
Figure 8. Significant effects of interaction between diagnosis and rs2254298 of OXTR with spatial map

Children with TD showed significantly increased resting functional connectivities compared to ASD children associated with the risk allele of rs2254298 in 4 ICs with spatial map: 3 CCs (C25, C13, and C21) and 1 DMN (C18). ($p < 0.05$ corrected for multiple comparisons using FDR)
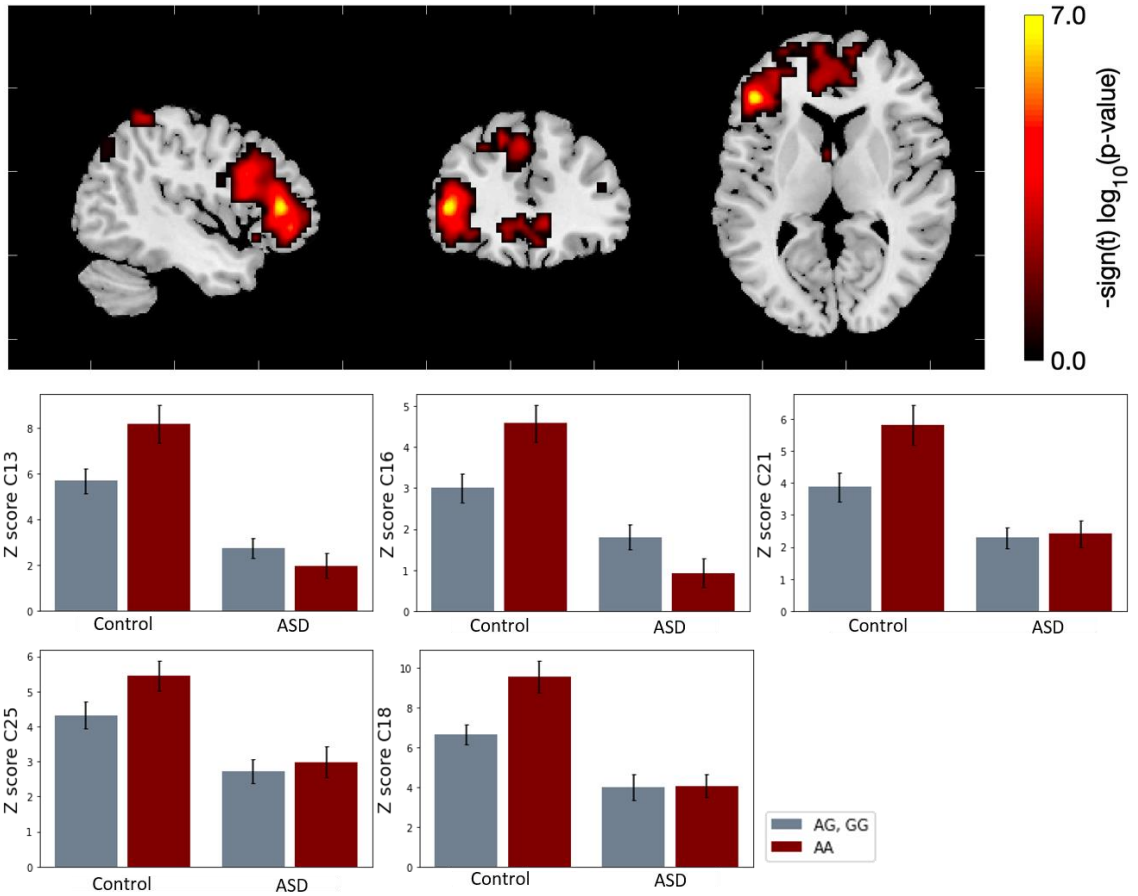
Figure 9. Significant effects of interaction between diagnosis and rs53576 of OXTR with spatial map

Children with TD showed significantly increased resting functional connectivities compared to ASD children associated with the risk allele of rs2254298 in 5 ICs with spatial map: 4 CCs (C13, C16, C21 and C25) and 1 DMN (C18). ($p < 0.05$ corrected for multiple comparisons using FDR)
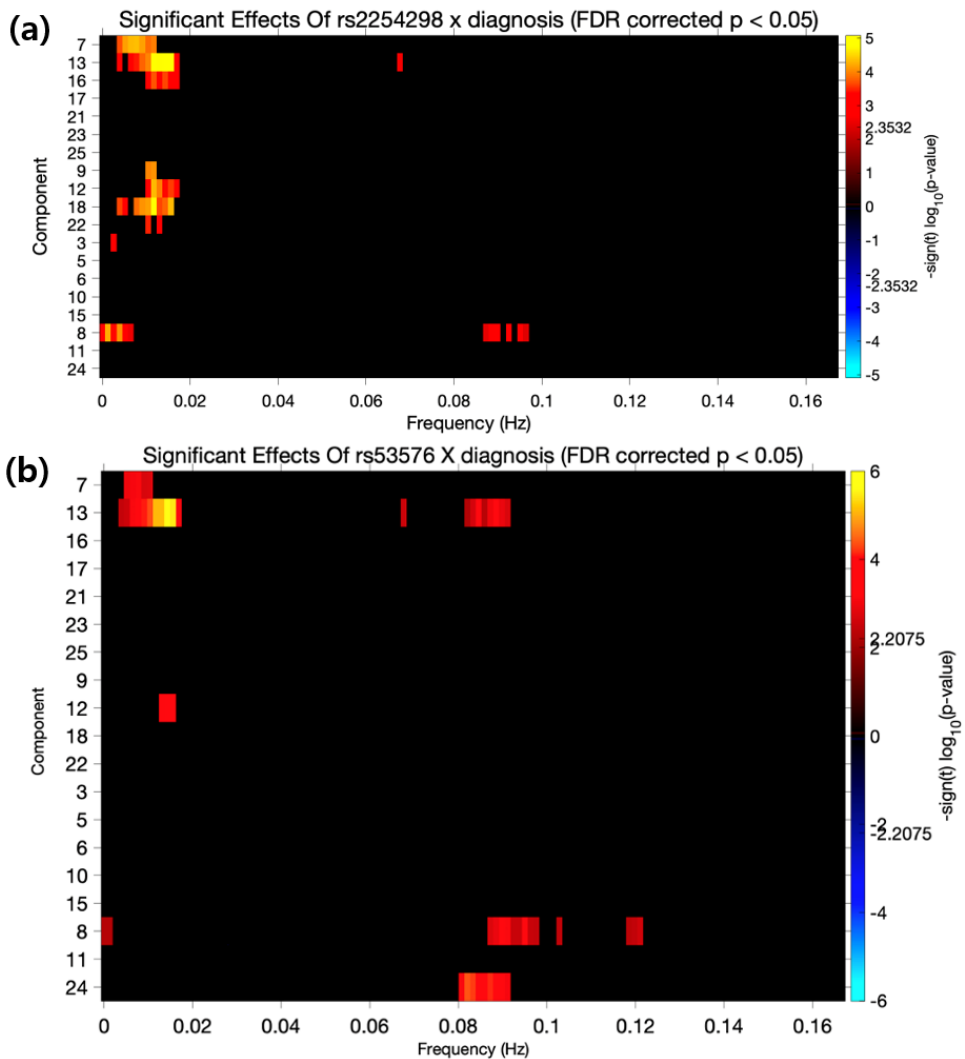
Figure 10. Significant effects of interaction between diagnosis and rs2254298 (a) and rs53576 (b) of OXTR with time course spectra

(a) In total, 8 ICs (4 DMNs [C9, C12, C18, and C22], 2 CCs [C13 and C16], 1 AUD [C7], and 1 SM [C3]), children with TD showed significantly greater spectral power (colored bins with orange, yellow, and red) associated with the risk allele of rs2254298. (b) 5 ICs (1 DMN [C12], 1 CC [C13], 1 AUD [C7], and 2 VIS [C8 and C24]), children with TD showed significantly greater spectral power associated with the risk allele of rs53576 ($p < 0.05$ corrected for multiple comparisons using FDR).

Effects of the methylation level of OXTR on resting-state functional connectivity

Since there was a difference in the number of subjects in the epi-genetic imaging analysis, 40 in the ASD group and 40 in the TD group, the visual inspection and selection of the ICs were newly carried out (Figure 11). In the analysis of the interaction between diagnosis and methylation level of CpG site 924 (pos1), significant differences were observed in two FNCs: CC-SUB and DMN-SUB networks (Figure 12). In both FNCs, resting FCs increased as the methylation of CpG site 924 increased in the TD group, whereas hyper-methylation was associated with a decrease in FCs in the ASD group.

In the spatial map analysis, there was a significant difference in the interaction effect between diagnosis and methylation level of CpG site 934 (pos 2) in one IC of the SM network (Figure 13). In the control group, as methylation level increased, the connectivity strength increased, whereas the strength of connectivity was significantly lower in the ASD group.

Finally, we evaluated the change in spectral power according to the level of methylation in the two groups. Regarding methylation level of CpG site 934, there were significant differences between groups in both low and high frequencies in one IC (CC network [C 14]) (Figure 14). At low frequencies, as methylation level increased, the TD group showed stronger connectivity than the ASD group, and the opposite result was observed at high frequencies.

In addition, we tested the effect of methylation on rs-FC, a significant decrease in FC was observed with increasing methylation of CpG site 924 in one FNC (SM-SM [C2-C16]) and five spatial map measures (3 CCs [C19, C20, and C25] and 2

DMNs [C18 and C22]) (Figure 15 and 16).

Unfortunately, we could not find any clinical correlation regarding the alterations in FC values based on the methylation of the OXTR in ASD children.
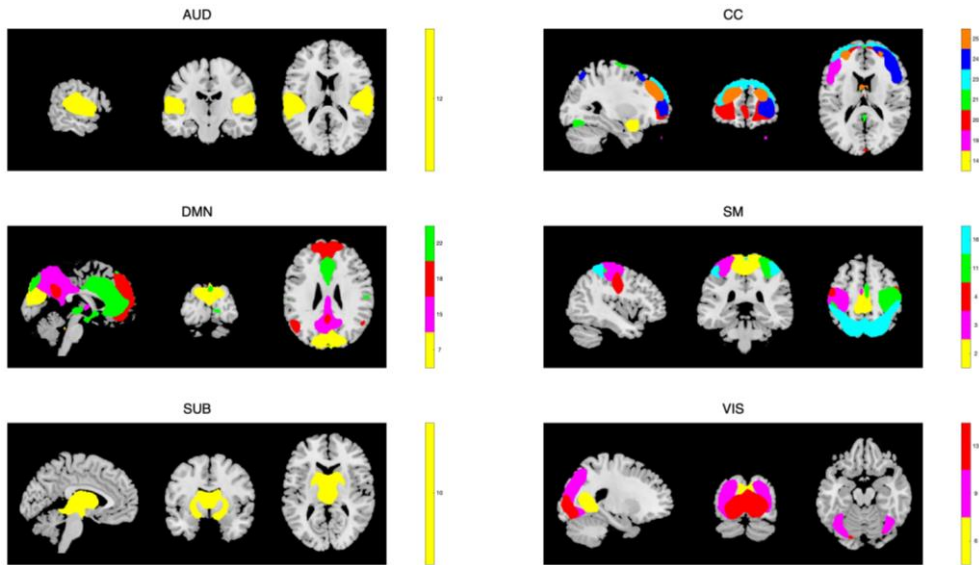
Figure 11. ICs generated from visual inspection of spatial maps associated with the imaging epigenetics of OXTR All the selected ICs (n = 21) were arranged using intrinsic networks. The component spatial maps are shown in color (t ≥ 1).

*Abbreviations: IC, independent component; CC, cognitive control; DMN, default mode network; AUD, auditory; SM, somatomotor; SUB, subcortical; VIS, visual
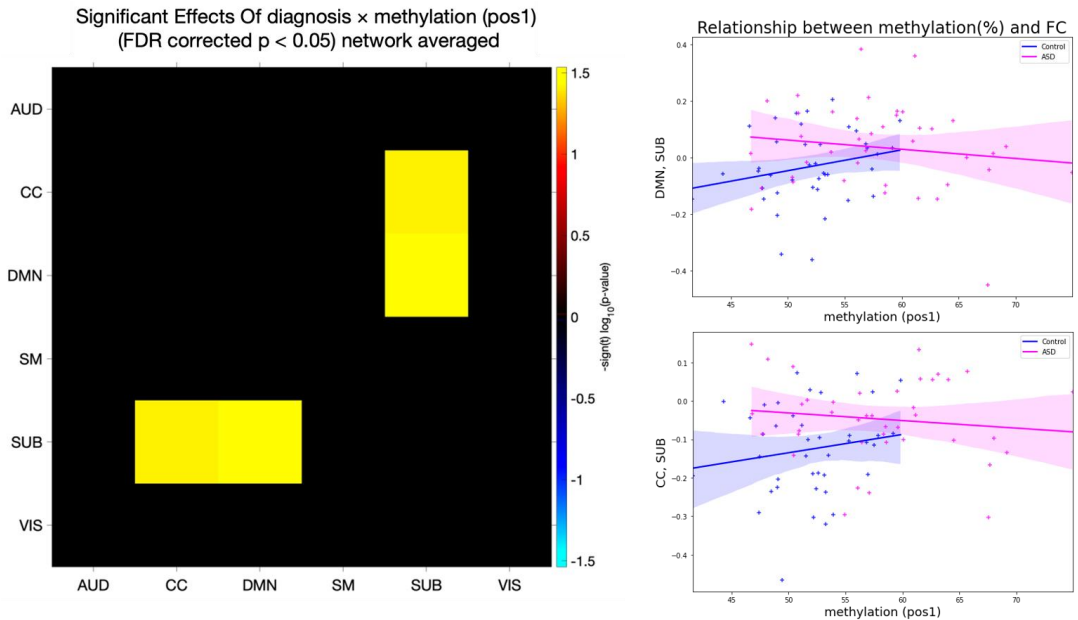
Figure 12. Significant effects of interaction between diagnosis and methylation level of OXTR (CpG site 924, pos 1) with FNC (network-wise analyses)

In CC-SUB and DMN-SUB networks, FNCs increased as the methylation level increased in the TD group (blue), whereas connectivity reduced as the methylation level increased in the ASD group (pink) ($p < 0.05$ corrected for multiple comparisons using FDR).
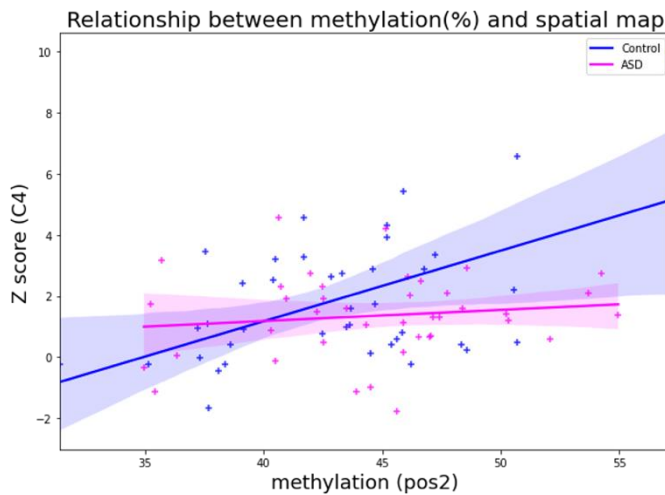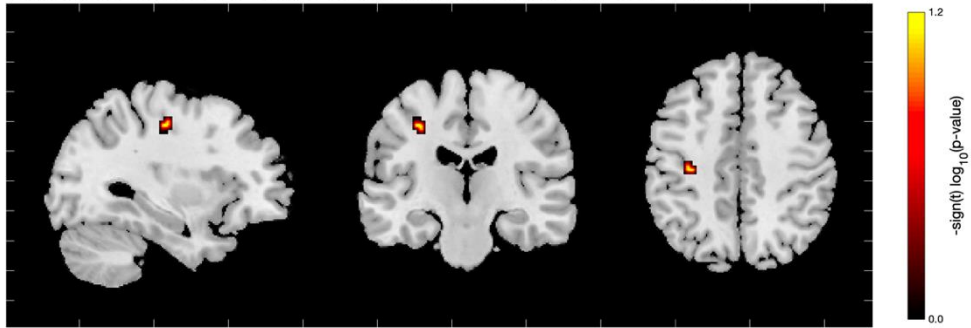
Figure 13. Significant effects of interaction between diagnosis and methylation level of OXTR (CpG site 934, pos 2) with spatial map

In a SM network (C4) Children with TD showed significantly increasing resting functional connectivities compared to ASD children associated with the hyper-methylation of the CpG site 934 ($p < 0.05$ corrected for multiple comparisons using FDR).
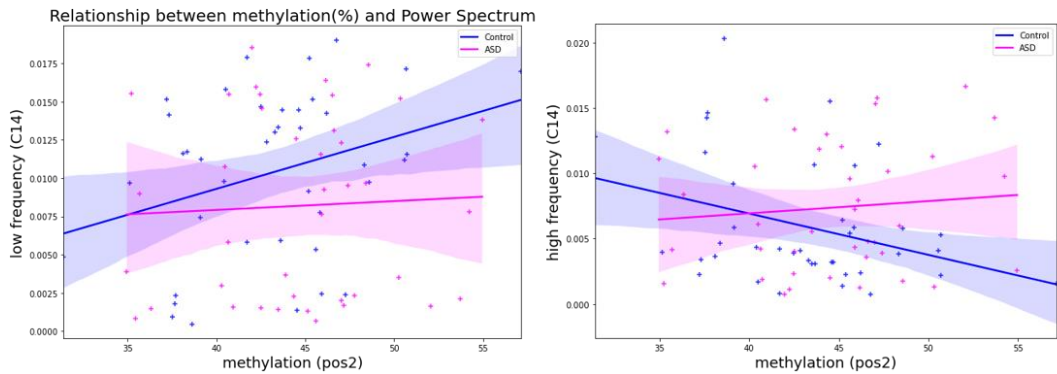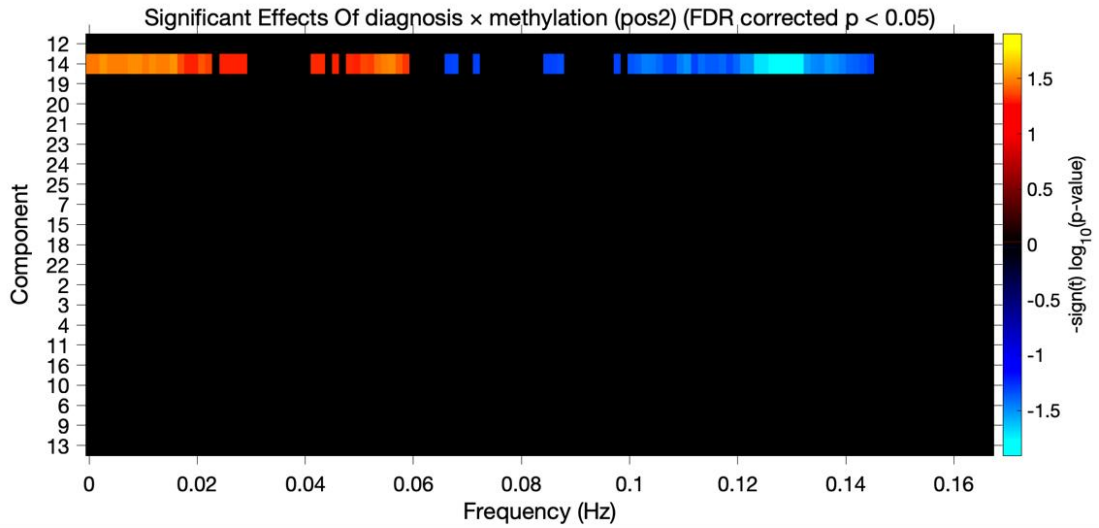
Figure 14. Significant effects of interaction between diagnosis and methylation level of OXTR (CpG site 934, pos 2) with time course spectra

In a IC of CC network (C 14), at low frequencies, as methylation level increased, the TD group showed stronger connectivity than the ASD group. On the contrary, at high frequencies, as the methylation level increased, the spectral power significantly decreased in TD group compared to the ASD group ($p < 0.05$ corrected for multiple comparisons using FDR).
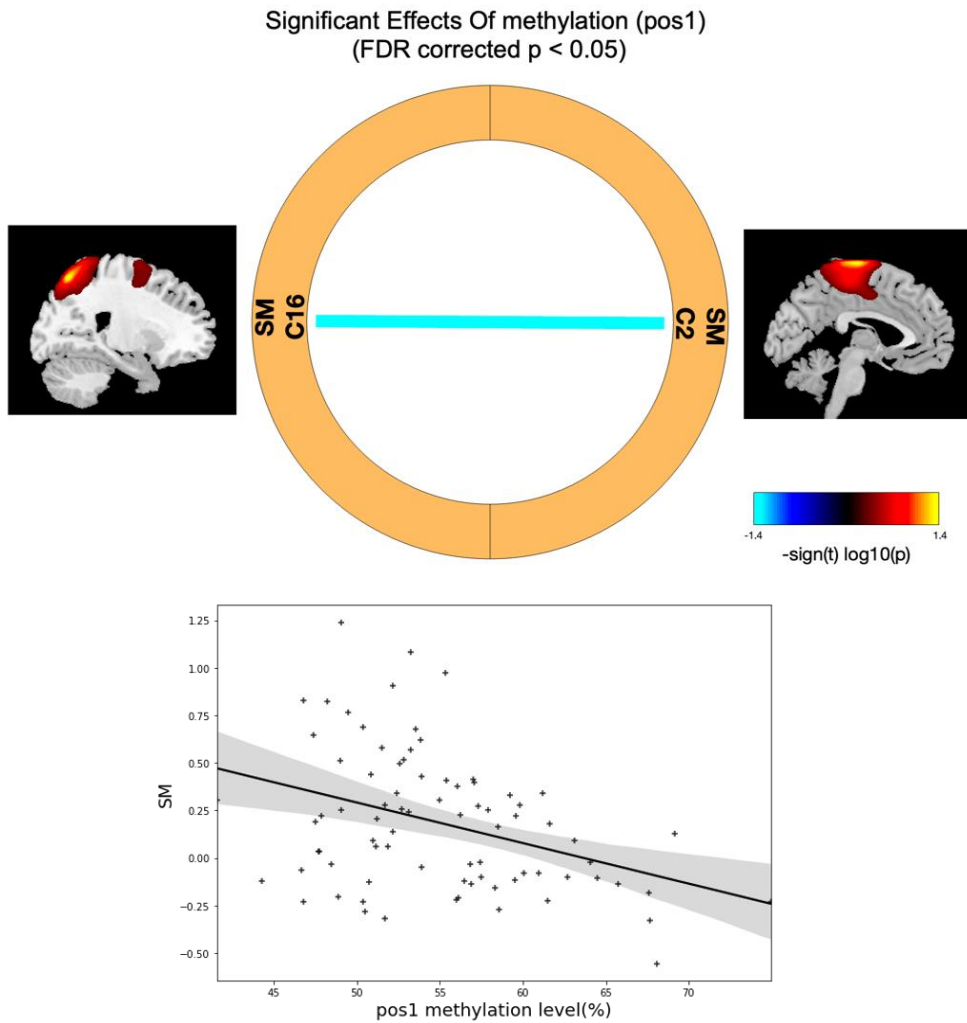
Figure 15. Significant effects of the methylation of OXTR (CpG site 924, pos 1) on FCs with FNC A significant decrease in FC was observed with increasing methylation of CpG site 924 in one FNC (SM-SM [C2-C16])).

*Abbreviations: SM, somatomotor; FDR, false discovery rate
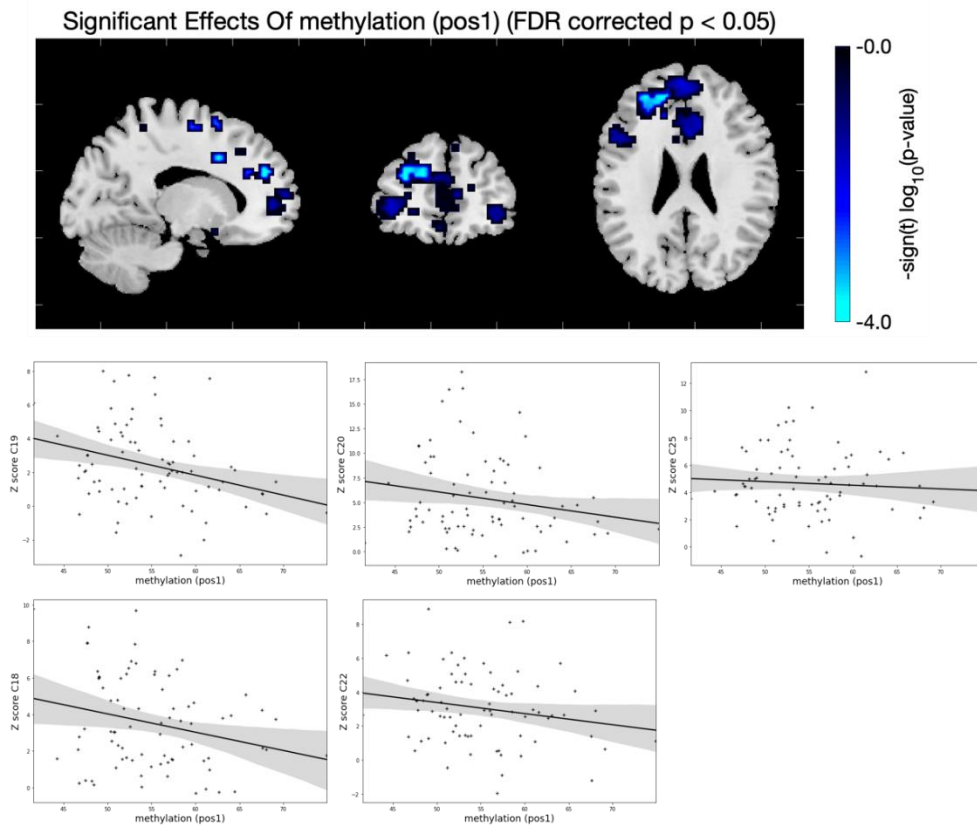
Figure 16. Significant effects of the methylation of OXTR (CpG site 924, pos 1) on FCs with spatial map There were five spatial map measures (3 CCs [C19, C20, and C25] and 2 DMNs [C18 and C22]) showing significant decreases in FC associated with increasing methylation of CpG site 924.

*Abbreviations: FDR, false discovery rate

Clinical correlations in imaging genetics and epi-genetics of OXTR

In correlation analyses with measures of imaging genetics and several clinical scores, we observed several significant results (Table 8). Among the ICA results of rs2254298, the FNC between IC 17 (CC) and IC 25 (CC) showed significant negative correlations with communication sub-score of ADOS and CSS in children with ASD. For rs535876, significant correlations were found between three aberrant FNCs (CC-CC [C16-C17], DMN-CC [C22-C23], and SM-CC [C6-C16]) and clinical scores including ADOS, CARS, and SRS. No statistically significant correlation was observed in other measures of imaging genetics. The epi-genetic imaging analysis results did not reveal any correlation with the autism clinical scores.

In addition, the analysis results of the differences in clinical scores according to genotypes of the two SNPs (rs2254298 and rs53576) are presented in Table 9 and 10. The full results of the clinical correlation analysis of imaging genetics are shown in the Table 11 and 12.

Table 8. Significant results of correlation analyses on FNC for two SNPs (rs2254298 and rs53576) of OXTR and clinical scores in children with ASD

Outcome measurements		Clinical correlation	
		Pearson corr (r)	Sig (p)
FNC (rs2254298)			
IC17, IC25	**ADOS_com**	-0.342	0.033
	CSS	-0.373	0.021
FNC (rs53576)			
IC17, IC25	**ADOS_com**	-0.320	0.047
	CSS	-0.353	0.030
IC22, IC23	**ADOS_socint**	-0.318	0.049
	ADOS_behav	-0.379	0.017
	ADOS_tot	-0.393	0.013
	CARS	-0.368	0.019
IC6, IC16	**SRS_awa**	-0.452	0.002

Abbreviations: IC, independent component; ADOS, Autism Diagnostic Observation Schedule; com; communications; CSS, Calibrated Severity Score; socint, social interaction; behave, restricted and repetitive behaviors; tot, total; CARS, Childhood Autism Rating Scale; SRS, Social Responsiveness Scale; awa, social awareness

Table 9. Differences in ADOS scores according to genotype of rs2254298 and rs53576 in children with ASD

Variables	rs2254298			rs53576		
	AA + AG (n = 19)	GG (n = 20)	P - value	AA (n = 15)	AG + GG (n = 24)	P - value
ADOS_com	5.105 (1.696)	5.95 (1.904)	0.153	4.867 (1.727)	5.958 (1.805)	0.07
ADOS_socint	10.105 (2.447)	10.650 (2.323)	0.48	9.733 (2.219)	10.792 (2.413)	0.178
ADOS_behav	1.684 (1.455)	1.950 (1.234)	0.541	1.533 (1.506)	2.0 (1.216)	0.294
ADOS_tot	16.947 (3.704)	18.550 (4.136)	0.211	16.2 (3.726)	18.750 (3.859)	0.049
CSS	7.053 (1.649)	7.737 (1.593)	0.202	6.733 (1.580)	7.826 (1.557)	0.043

Abbreviations: Autism Diagnostic Observation Schedule; com; communications; CSS, Calibrated Severity Score; socint, social interaction; behave, restricted and repetitive behaviors; tot, total

Table 10. Interaction effect between group and genotype of rs2254298 and rs53576 in clinical scores

Variables	rs2254298		rs53576	
	F	**P -value**	**F**	**P -value**
CARS	3.064	0.084	0.475	0.493
SRS_awa	0.589	0.446	0.059	0.809
SRS_cog	0.128	0.722	0.360	0.551
SRS_com	0.335	0.565	0.128	0.722
SRS_mot	3.940	0.053	2.198	0.144
SRS_res	1.648	0.205	0.076	0.784
SRS_sci	0.679	0.414	0.112	0.739
SRS_tot	0.993	0.324	0.113	0.739

Abbreviations: CARS, Childhood Autism Rating Scale; SRS, Social Responsiveness Scale; awa, social awareness; cog, social cognition; mot, social motivation; res, restricted interests and repetitive behaviors; sci, social communications index; tot, total

Table 11. Results of correlation analyses on FNC for genotype of rs2254298 of OXTR and clinical scores in children with ASD

		ADOS_com	ADOS_soc	ADOS_beh	ADOS_tot	ADOS_css	CARS	SRS_awa	SRS_cog	SRS_com	SRS_mot	SRS_res	SRS_sci	SRS_tot
IC17, IC25	Pearson corr (r)	-.342*	-0.151	-0.029	-0.265	-.373*	0.135	-0.149	0.126	-0.027	-0.006	-0.009	-0.012	-0.011
	Sig (p)	0.033	0.360	0.863	0.104	0.021	0.405	0.448	0.523	0.892	0.975	0.964	0.953	0.954
IC17, IC13	Pearson corr (r)	0.092	-0.184	0.025	-0.051	0.066	0.186	-0.193	-0.077	-0.180	-0.050	-0.275	-0.152	-0.190
	Sig (p)	0.578	0.263	0.882	0.756	0.693	0.252	0.325	0.697	0.359	0.799	0.156	0.439	0.333
IC17, IC23	Pearson corr (r)	0.017	-0.094	-0.017	-0.054	0.074	0.164	0.060	0.080	0.194	0.242	-0.021	0.181	0.134
	Sig (p)	0.919	0.571	0.917	0.742	0.660	0.312	0.762	0.686	0.322	0.215	0.915	0.356	0.498
IC5, IC16	Pearson corr (r)	-0.007	0.014	-0.301	-0.097	-0.004	-0.106	-0.052	-0.074	-0.083	0.180	-0.007	-0.024	-0.021
	Sig (p)	0.966	0.930	0.063	0.558	0.983	0.516	0.794	0.709	0.675	0.360	0.973	0.902	0.918
IC12, IC18	Pearson corr (r)	0.012	0.180	0.199	0.170	0.170	0.290	0.259	0.258	0.312	0.269	0.058	0.323	0.264
	Sig (p)	0.943	0.273	0.224	0.301	0.308	0.069	0.184	0.184	0.106	0.166	0.768	0.094	0.175
IC5, IC11	Pearson corr (r)	0.299	-0.121	0.148	0.124	0.075	0.222	-0.214	0.095	-0.039	-0.006	-0.079	-0.036	-0.049
	Sig (p)	0.064	0.464	0.368	0.451	0.653	0.169	0.275	0.629	0.844	0.977	0.689	0.855	0.805
IC10, IC11	Pearson corr (r)	0.059	-0.070	-0.015	-0.020	0.119	0.167	-0.119	-0.349	-0.297	0.104	-0.333	-0.223	-0.260
	Sig (p)	0.720	0.672	0.930	0.905	0.478	0.303	0.546	0.069	0.125	0.599	0.084	0.253	0.182
IC11, IC16	Pearson corr (r)	0.151	0.069	0.123	0.161	0.126	0.158	-0.197	-0.113	-0.076	0.042	-0.209	-0.089	-0.124
	Sig (p)	0.360	0.678	0.457	0.326	0.450	0.331	0.315	0.568	0.702	0.832	0.285	0.653	0.530

Table 12. Results of correlation analyses on FNC for genotype of rs53576 of OXTR and clinical scores in children with ASD

		ADOS_com	ADOS_soc	ADOS_beh	ADOS_tot	ADOS_css	CARS	SRS_awa	SRS_cog	SRS_com	SRS_mot	SRS_res	SRS_sci	SRS_tot
IC5, IC16	Pearson corr (r)	0.030	-0.011	-0.278	-0.086	-0.016	-0.023	-0.142	-0.167	-0.173	0.086	-0.129	-0.128	-0.133
	Sig (p)	0.856	0.945	0.086	0.604	0.925	0.890	0.471	0.394	0.380	0.662	0.512	0.515	0.500
IC6, IC16	Pearson corr (r)	-0.115	-0.185	-0.150	-0.212	-0.228	-0.079	-.516**	-0.347	-0.310	-0.078	-0.221	-0.344	-0.323
	Sig (p)	0.486	0.260	0.363	0.195	0.169	0.628	0.005	0.071	0.108	0.692	0.258	0.073	0.094
IC17, IC25	Pearson corr (r)	-.320*	-0.141	0.009	-0.232	-.353*	0.133	-0.134	0.080	-0.017	-0.080	-0.040	-0.032	-0.035
	Sig (p)	0.047	0.392	0.959	0.156	0.030	0.412	0.497	0.686	0.933	0.685	0.839	0.870	0.858
IC5, IC24	Pearson corr (r)	0.031	0.049	-0.172	-0.011	0.063	-0.186	-0.118	-0.206	-0.191	-0.009	-0.270	-0.165	-0.198
	Sig (p)	0.853	0.769	0.294	0.947	0.707	0.252	0.549	0.292	0.330	0.964	0.165	0.401	0.311
IC9, IC24	Pearson corr (r)	0.260	0.188	0.145	0.278	0.093	.522**	0.031	-0.042	0.074	0.055	-0.018	0.044	0.029
	Sig (p)	0.110	0.252	0.378	0.087	0.579	0.001	0.875	0.831	0.710	0.782	0.927	0.823	0.883
IC22, IC25	Pearson corr (r)	-0.139	-0.147	-0.096	-0.196	-0.206	-0.067	0.071	0.176	-0.002	-0.061	-0.035	0.039	0.021
	Sig (p)	0.399	0.371	0.560	0.231	0.215	0.681	0.718	0.370	0.993	0.759	0.859	0.843	0.916
IC22, IC23	Pearson corr (r)	-0.153	-.318*	-.379*	-.393*	-0.267	-.368*	-0.182	0.040	-0.151	-0.224	-0.077	-0.150	-0.135
	Sig (p)	0.352	0.049	0.017	0.013	0.105	0.019	0.354	0.839	0.443	0.251	0.699	0.447	0.492

IC22, IC7	Pearson corr (r)	0.032	0.180	-0.117	0.085	0.192	0.126	-0.031	0.083	-0.002	0.038	0.050	0.022	0.030
	Sig (p)	0.848	0.274	0.480	0.606	0.247	0.439	0.874	0.676	0.993	0.850	0.800	0.912	0.879
IC6, IC21	Pearson corr (r)	0.235	0.176	0.057	0.232	0.272	0.070	0.055	-0.010	0.226	0.275	0.168	0.182	0.184
	Sig (p)	0.150	0.283	0.731	0.154	0.099	0.667	0.783	0.958	0.248	0.157	0.393	0.354	0.347
IC16, IC17	Pearson corr (r)	-0.221	0.100	-0.081	-0.073	-0.063	-0.009	0.048	0.113	0.168	0.127	0.185	0.147	0.162
	Sig (p)	0.175	0.543	0.624	0.660	0.707	0.957	0.808	0.569	0.392	0.521	0.346	0.456	0.410
IC5, IC15	Pearson corr (r)	0.102	0.066	0.009	0.101	0.099	0.159	-0.060	-0.238	-0.080	-0.087	-0.173	-0.126	-0.143
	Sig (p)	0.536	0.691	0.954	0.539	0.553	0.327	0.763	0.223	0.686	0.660	0.378	0.522	0.468
SM_CC	Pearson corr (r)	0.081	0.172	-0.038	0.120	0.063	0.015	-0.169	0.028	0.007	0.192	0.077	0.025	0.040
	Sig (p)	0.626	0.294	0.818	0.465	0.706	0.928	0.391	0.886	0.973	0.328	0.698	0.900	0.842
SM_VIS	Pearson corr (r)	0.063	-0.071	0.100	0.027	0.158	.324[*]	-0.098	-0.021	-0.191	0.039	-0.133	-0.106	-0.117
	Sig (p)	0.705	0.669	0.544	0.873	0.343	0.042	0.619	0.917	0.331	0.843	0.498	0.592	0.554
SUB_SM	Pearson corr (r)	-0.004	0.034	-0.003	0.026	0.049	0.019	0.079	-0.023	0.023	0.074	0.016	0.038	0.033
	Sig (p)	0.979	0.839	0.987	0.877	0.772	0.910	0.691	0.909	0.907	0.709	0.935	0.850	0.867
SUB_VIS	Pearson corr (r)	0.022	-0.038	0.021	-0.006	0.063	0.196	0.146	0.139	0.102	0.022	0.191	0.114	0.138
	Sig (p)	0.895	0.819	0.900	0.972	0.707	0.226	0.458	0.482	0.605	0.910	0.329	0.563	0.482

Discussion

Decreased functional connectivities in children with autism spectrum disorder (ASD)

Children with ASD showed significantly lower values of the spatial map compared with TD children in most DMN and CC network components, and these results were similarly observed in the FNC analysis. Lower intrinsic FC in children with ASD than in TD children has been repeatedly reported in previous studies (52-55), and reduced FC values have been considered to decrease the synchronization of neuronal activity in brain regions (55). In addition, aberrant synchronized activation between several brain regions underlies the varied deficits associated with specific impairments in ASD (56-58). In particular, as most participants in the ASD group were individuals with low-functioning autism with intellectual disabilities, we expected decreased FC of cognitive function-related brain areas, including social cognition, in the ASD group and observed consistent results with expectations.

The DMN is a key brain system related to social cognition, processing information about the self and others (59-61). Impairment of social function is one of the core symptoms of autism, and aberrant function of the DMN is related to deficits in social cognition in ASD (62). We observed decreased FC in several brain areas of the DMN, including the PCC, anterior cingulate cortex, angular cortex, medial prefrontal cortex (mPFC), precuneus, and cuneus, in children with ASD compared with TD children. In particular, the PCC, precuneus, and mPFC are

implicated in self- and other-relevant processing (62), including self-referential and autobiographical processing (63-65), and monitoring of mental states of oneself and others (64, 66). As described above, studies on the aberrant intrinsic FC of the DMN have been steadily conducted, but findings about under-/over-connectivity in the resting brain have been inconsistent. In a 2019 meta-analysis, reduced resting-state FC of the DMN, including the PCC, was reported in children with ASD compared with TD children (11). However, several studies on intrinsic FC in individuals with ASD have reported both over- and under-connectivities (67-72). In this study, we only observed under-connectivities of the DMN-related FCs, and these results are meaningful in that this study was targeted in a relatively younger ASD group with severe functional deficits.

In addition, we observed decreased FC between the DMN and sensory-related networks, such as the VIS and AUD networks. A previous fMRI study reported that decoupling of the DMN and VIS network was associated with decreased attention in text reading (73). Another study reported reduced FC between the DMN and the visual region in children with ASD and discussed social visual engagement difficulties, one of the characteristics of ASD (74). Studies on reduced connectivity between the DMN and AUD network explained this in relation to the decreased response to human voice and the functional deficit of communication skills (75, 76). Similar to previous studies, the under-connectivity between the DMN and sensory-related cortex observed in this study is thought to be related to the reduced function of the social brain associated with aberrant sensory perception in ASD.

In this study, we observed the largest number of under-connectivity values in the frontal and parietal regions, which were classified as CC network components.

In addition to the social cognition mentioned above, individuals with ASD have difficulties in various cognitive domains, including executive function (77), working memory (78), language processing/learning (79, 80), processing speed (81), and attention (82). In particular, the fronto-frontal and fronto-parietal networks, where the most evident decreases were observed in this study, play central roles in CC (83). Decreased fronto-parietal connectivity has also been suggested to be critically associated with difficulties in executive functioning (84), working memory (85), and attention (86) in ASD. As the ASD group in this study included individuals with ASD with severe functional decline accompanied by intellectual disability, the decrease in FC of the brain network related to cognitive function would have been more prominent. Our findings demonstrate the aberrant development of cognitive function-related brain regions in children with ASD and support the need for early interventions, including nonsocial cognitive domains and social cognition.

Decreased FC in children with ASD has been significantly correlated with several clinical scores. In particular, we observed negative correlations between brain networks, such as the CC network and DMN, and the clinical scores of ADOS and SRS, suggesting that the reduced FC of the brain region related to social/nonsocial cognition affects the manifestation of ASD phenotypes. In one IC of Spatial map (C25) (Figure 2), as FC decreased, the communication sub-score and CSS of ADOS increased, suggesting that decreased superior frontal connectivity related to cognitive function was associated with worsening communication symptoms in autism. Also, in several ICs of FNC (4 CCs [C13, C16, C17, and C23], 1 DMN [C22], 1 SM [C5], and 1 VIS [C24]), it was inferred that the under-connectivity of resting networks was associated with worsening autistic symptoms

such as deficits of communication, social interaction, social awareness, and repetitive and restricted behaviors (Table 4 and Figure 3).

Increased functional connectivities in children with ASD

In results of spatial map analyses, one IC in the SUB network region and two ICs in the VIS network region showed stronger FC in children with ASD than in TD children. Interestingly, these findings are similar to those of the FNC analysis. In children with ASD, the FC between the IC, including the right thalamus, and the IC, including the visual areas, such as the cuneus, lingual gyrus, and middle occipital gyrus, was significantly higher compared with TD children. In addition, the FC between the SUB and SM network regions within the frontal lobe was also significantly higher in the ASD group than in the TD group. These are significantly contrary and interesting results compared with the discussion above, which mainly addressed the under-connectivity of the FC associated with cognitive functions, such as executive function and social cognition in ASD. There are several previous studies on aberrant FC of the SUB network area, including the thalamus, in ASD, and several studies have reported findings consistent with the results of this study (87-89). In 2019, Maximo and Kana (90) explored deep brain connectivity in ASD using data from the Autism Brain Imaging Data Exchange, and similar to this study, they reported over-connectivities between SUB network regions and sensory-related cortical areas and under-connectivities between subcortices and cognition-related cortices.

The thalamus functions as an integrated hub in the functional brain network that gates afferent sensory input to the cortex, modulates efferent motor signals, and,

consequently, regulates overall cortical activity (89, 91). Altered sensory processing is one of the most typical phenotypes of ASD, and previous studies have suggested that aberrant thalamocortical connectivity is a potential cause (92). During normal development, brain networks develop in a way that is not overly affected by sensory stimuli for processing higher-order cognitive functions, which can be assumed as a process of increased independence of the cortical connectivity from the sensory inputs from the subcortices (87, 93, 94). The abnormal subcortico-cortical FC observed in children with ASD reflects delayed or immature neurodevelopment, which is consequently associated with deficits in higher-order cognitive function and sensory processing.

Unusual visual perception is one of the most common symptoms in children with ASD, and in clinical settings, we often encounter children with ASD who have visual seeking behavior while staring at specific objects (e.g., ceiling fans or wheels of toy cars) remarkably closely for a long time or who are extensively resistant to everyday light. They are expected to have different processes in receiving and processing visual stimuli from TD children and possibly have deficits in filtering unwanted or irrelevant sensory stimuli at the subcortical level (93). In this study, we found atypically increased FNC between the thalamus and visual cortices, including the cuneus, which plays a role in both primary and secondary visual processing (95). In future studies, we can obtain further information on neurodevelopmental abnormalities related to visual sensory processing in children with autism by exploring more detailed brain regions or investigating age-specific changes.

In children with ASD, we also found over-connectivity between the SUB and somato-motor components, including the pre- and post-central gyri. The pre- and

post-central gyri are brain areas mainly responsible for the execution of motor commands and perception of sensory stimuli, respectively (96). Similar to visual perception, several individuals with ASD have somatosensory deficits, such as hyper-/hypo-sensitivities (97, 98) and/or unusual seeking behavior for tactile stimuli (99). Although not all children with ASD have motor symptoms, several studies have reported motor deficits in ASD, such as motor incoordination (100, 101) and gross and fine motor impairments (102). In fact, several previous studies have reported abnormalities in connectivities between the thalamus and sensorimotor cortical regions in ASD (88, 89, 96, 103), and most studies have reported results consistent with the findings of the current study.

We observed positive correlations between the subcortico-visual FC and clinical scores of the ADOS and awareness domain of the SRS (Table 4). Even when the FNC analysis was performed by simplifying the classification of the components, significant positive correlations were observed between the FC of SUB–VIS networks and several sub-scores of the SRS (Table 4). In other words, the stronger the FC, the worse the symptoms of autism including social functional impairments and restricted interests and repetitive behaviors. Therefore, we can infer that the abnormal over-connectivity between the thalamus and visual brain regions is associated with the expression of ASD phenotypes.

Aberrant functional connectivities in children with ASD associated with genetic variants of oxytocin receptor gene (OXTR)

We could not found genotypic differences between the two group in both OXTR SNPs (rs2254298 and rs53576), and it is inferred to be due to the relatively small number of subjects in this study. Most studies exploring OXTR genotype differences included 200 to 400 or more subjects (28), and a study on the effective sample size of genetic analysis reported that the mean size ranged between 237 and 1784 (104). Nevertheless, ASD children showed significantly different aberrant FC from TD children according to the OXTR genotypes. The FNC results of rs2254298 indicate that the discrepancy in connectivity between brain regions that were decreased in ASD compared to TD became more apparent in the risk allele carriers (Figure 5). The effect of rs2254298 risk genotypes was most prominent in the CC networks (C25, C17, C13, C23, and C16) which mainly included the superior and middle frontal gyri, cingulate gyrus (CG), and superior and inferior parietal lobules (SPL and IPL). In addition to the CC networks, results in the same direction were observed in the DMN networks (C18 and C12), SM networks (C5 and C10), and VIS network (C11). As mentioned above, DMN networks included brain areas related to the social cognition, such as precuneus, PCC, CG, and IPL. SM networks included somatosentory-related areas including precentral and postcental gyri, and VIS networks included several occipital areas, cuneus, and precuneus etc.

The results of this study were consistent with earlier research of the imaging genetics, which demonstrated that individuals with typical development who had genetic variations of ASD-risk gene showed atypical function and structure of their brains (105-107). In association with rs2254298 A allele, there was a previous study on the decline of dorsal anterior cingulate gyrus function during emotion processing in healthy adult subjects (33). Another previous study reported significantly lower

rsFC of the DMN area in A carriers of rs2254298 compared to GG genotyped healthy subjects (108). Most imaging genetic studies on OXTR have reported results of reduced FC associated with alleles, implying that the presence of risk allele inhibits OXTR expression, resulting in lowered neurological activity and FC. OXTR is classified as a G-protein coupled receptor which affects neural excitability through cascade reactions (109). Therefore, changes in neural activities by OXTR variants in the brain areas may have caused reduced FC in those brain regions. Interestingly, in our findings, these alterations by the risk allele of the OXTR gene reduced intrinsic connectivities only in ASD children, and in contrast, increased FC in the TD children. Our findings of these differences between the two group can be explained by the possibility that in typical development, there is a mechanism to compensate for the increased genetic risk, but the same compensatory process does not occur in the ASD children. In a prior imaging genetic study of OXTR targeting ASD, the authors explored the additive effects of the risk allele (A) in OXTR SNPs including rs2254298 (107). Similar to our findings, the results of this study showed opposite changes according to the risk allele between ASD and control groups. In the ASD group, as the risk allele dosage increased, the connectivity of the network including the nucleus accumbens (NAcc) and anterior cingulate gyrus (ACG) decreased, whereas the connectivity of the frontal region increased in the control group. These crossover effects between the ASD group and the control group showed similar results in a study conducted by Uzefovsky et al. in 2019 (110). The authors reported that the A carrier of rs2254298 in the ASD group showed hypoactivity in the right supramarginal gyrus and the right inferior parietal lobule region, whereas the control group showed the opposite result.

In the FNC results of rs53576, we observed similar findings in direction of FCs to those of rs2254298 in several brain regions. Among a total of 11 FNCs presenting significant interaction effects of diagnosis and genotype, in 7 FNCs, ASD showed reduced FCs associated with A allele, and TD showed strengthened FCs, resulting in a greater difference between the two groups (Figure 6) (1 CC-CC [C16-C17], 1 DMN-CC [C22-C23], 3 CC-SMs [C16-C5, C16-C6, and C21-C6], 1 DMN-AUD [C22-C7], and 1 SM-VIS [C5-C24]. Previous studies on rs53576 of OXTR in healthy subjects also reported a decrease associated to the A allele in the FC of areas related to the limbic system such as amygdala, hypothalamus, and NAcc (29, 107, 111). In three other FNCs (CC [C17] – CC [C25], DMN [C22] – CC [C25], and DMN [C9] – VIS [C24]), risk allele (A) acted in the direction of increasing the difference between the two groups, but both groups were equally strengthened in FC. However, in the results of the rs52576 analysis, we also observed the aberrant over-connectivity in ASD children found in the subcortical area when comparing between groups above. In contrast to other brain areas, the FNC between SUB-SM (C15-C5) showed lower connectivity in the TD group compared to ASD group, and the risk allele of rs53576 lowered the FC in the TD group and increased the FC in the ASD group, resulting in a wider difference between the two groups. The same result was found in the network-wise analysis calculated from the average value of components in each area, and in the network-wise results, we further found enhanced FC of SUB-VIS network in addition to SUB-SM (Figure 7). As mentioned earlier, the atypical over-connectivity of the subcortico-cortical area seen in the ASD group has been interpreted as a failure of the segregation process of the primary sensory region from the deep brain nuclei of the normal development process (90, 93). To the best of our

knowledge, no prior research has been conducted regarding the impacts of the OXTR gene on these immature brain developments in individuals with ASD. However, in this study, we discovered that the aberrant over-connectivity of subcortico-cortical network was reproduced, and moreover, we noted that this finding was amplified by the presence of the risk allele of OXTR gene. We believe that this discovery implies the significance of subcortico-cortical network and its susceptibility to OXTR gene in the atypical developmental process of ASD.

In the spatial map analysis, results were obtained mainly in the CC and DMN networks for both rs2254298 and rs53576 (Figure 8 and 9). The brain regions included in the ICs where significant differences were observed were mainly cognitive function-related networks including the several frontal regions such as orbital cortex, and the DMN such as the superior and middle frontal cortex and the ACC. Regarding the association of OXTR gene to the social function, previous studies were carried out about the effect of OXTR genetic variants on the activity of DMN, known as social brain (108, 112). The authors reported that individuals who carry the A allele of rs2254298 exhibited notably reduced rsFC in PCC and dorsal ACC in contrast to those with the GG genotype (108). Prior imaging genetic studies on OXTR have been focused on reward circuits such as limbic systems, but according to the results of our study, various brain regions related to social/nonsocial cognition that show major functional degradation in ASD are also likely to be affected by the OXTR.

We found significant correlations between clinical scores and FNCs that showed differences according to OXTR genotypes in the ASD group. The FNC between IC 17 and IC 25, which are cognitive related areas, showed negative

correlations with the communication subscore of ADOS and CSS in the results of the two SNPs. In can be interpreted that the decrease of FC in these regions associated with OXTR is related to the communication difficulties observed in ASD. For the rs53576, the decreased FNC between DMN (IC 22) and CC (IC 23) showed negative correlations with several subscores of ADOS including social interaction and repetitive behaviors. The reduced FC of DMN and CC networks in ASD was further decreased in association with the OXTR and also inferred to be related to the worsening of autism symptoms.

Aberrant functional connectivities in children with ASD associated with methylation of OXTR

In the findings of exploring the effect of methylation of OXTR gene on the intrinsic connectivity between ASD and TD groups, we observed the predicted result in two network-wise FNCs (SUB-DMN and SUB-CC) (Figure 12). The average value for the two FNCs was greater in the ASD group compared to the TD group, and as we previously discussed the abnormal over-connectivity of the subcortical region in individuals with ASD, it shall not be reiterated. In the imaging epigenetic analysis of this study, the hypermethylation of CpG site 924 (pos 1) induced a decrease in FC in the ASD group, which was the consistent finding with the previous studies (36, 113, 114). DNA methylation of the OXTR gene can lead to reduced gene expression and potentially altered oxytocin signaling in the brain and contribute to the decreased FC in social cognition related area observed in individuals with ASD (114). When we solely examined the impact of methylation on rs-FC, we observed a significant reduction in FC as the methylation levels of CpG site 924 increased

(Figure 15 and 16). However, in TD children, there was a positive correlation between methylation and FC strength, and this finding is consistent with the idea that increased connectivity may serve as a compensatory mechanism in response to genetic risk in TD group, as was observed in the imaging genetic analysis of this study.

We found a less clear but significant interaction effect between diagnosis and methylation level of CpG site 934 in one IC of SM network (C4) (Figure 13). The level of methylation at CpG site 934 (pos 2) was found to be strongly associated with increased connectivity in children with TD, but not in those with ASD, and this difference in the relationship between methylation and intrinsic FC was found to be statistically significant. As far as we know, there have been no previous studies investigating the impact of OXTR gene methylation on alterations in intrinsic connectivity in children with severe autism. However, based on the findings of this study, it is possible that increased methylation of OXTR could serve as a diagnostic marker especially in ASD children with profound symptoms, differentiating them from normally developing children.

Differences in the fluctuations of the intrinsic activity in children with ASD

This study also evaluated the ICs' spectra, providing the variations in intrinsic activity fluctuations (within the frequency range that fMRI data can capture). Previous studies have shown that low-frequency BOLD signals below 0.1 Hz are mainly considered to reflect the strength of brain activity in rs-fMRI analysis, and thus have been considered as an important characteristic in resting brain (115, 116).

High-frequency bands above 0.1Hz have been considered to be affected by physiological artifacts and have been evaluated as less important than low-frequency bands. However, recent studies have reported that BOLD signals of resting brain are observed from 0.1Hz or higher to up to 0.75Hz (117), and more recently, one study reported that the resting-state BOLD signal represents a frequency-specific network architecture for each frequency (118). Consistent with previous findings among individuals with mental disorders when compared with healthy controls (119), children with ASD displayed significant lower low-frequency power and higher high-frequency power compared with TD children (Figure 4). Our results, which indicate reduced low-frequency power and increased high-frequency power in children with ASD compared with TD children, are consistent with the finding of a previous longitudinal study. Agcaoglu et al. (2022) (120) found that the trend of significant rises in low-frequency power and significant declines in high-frequency power during normal development might indicate a general indicator of typical development in children. To the best of our knowledge, this is the first study to confirm that biomarkers of typical development are altered in an abnormal pattern in children with ASD.

The findings of the spectral power analysis of the two groups, with respect to the OXTR genotype, were observed similarly to the intergroup comparison above. Specifically, individuals carrying the A allele in the TD group exhibited an increase in spectral power in the low frequency range, while those in the ASD group showed a decrease in spectral power in the low frequency (Figure 10). This led to a widening of the difference between the two groups. In essence, the interaction effect between diagnosis and genotype was found to be statistically significant in multiple ICs.

While these results were observed in several ICs for both SNPs, the effect was more pronounced for rs224298 as compared to rs53576. However, in the high frequency range, no significant difference in spectral power could be obtained between the two groups associated with genotypes.

In spectra power analysis according to the level of methylation of the OXTR, we found a significant difference between the two groups in one IC (CC [IC14]) of the results of CpG site 934 (Figure 14). Although it was observed only in one IC, imaging epi-genetic analysis has better demonstrated the characteristic spectral power pattern of ASD children, which shows weaker spectral power in the low frequency and stronger spectral power in the high frequency as compared to TD children. The spectral power that changes with the level of methylation (%) in both groups can be seen in Figure 14 (lower graphs). It can be observed that the slope of ASD group does not change obviously, whereas the TD group shows a steep increase in low frequencies and a steep decrease in high frequencies. Consistent with the FNC results, it can be interpreted that compensatory processes for genetic risks occur in normal development, whereas such processes do not occur in development of ASD.

Limitations

This study has some limitations. First, the sedation effect could not be excluded from the results of the FC analysis. As mentioned above, most of the children in the ASD group and a smaller number of children in the TD group were sedated during the fMRI scan, and sedative agents may have affected fMRI results (121). The effects of sedation-induced changes in brain networks on fMRI signals are uncertain (122), making it more difficult to interpret differences in intrinsic networks. In future

studies, it will be necessary to exclude sedative effects and replicate the results. Second, although this study included relatively younger participants, the age range of the participants needs to be further subdivided. As childhood is a rapid period of brain development, it would be meaningful to divide participants between the ages of 2 and 12 years into a narrow range to observe the difference. However, as this study did not have sufficient participants for subdivision by age, we plan to explore the differences in FC according to a narrow age range in a larger sample in a follow-up study. In the same context, since the age and sex between the two group was significant, it is necessary to conduct an additional analysis in age- and sex-matched subjects in future studies. Third, there were some missing values in the clinical measures used in this study. Several significant associations were found between intrinsic connectivities and clinical symptom scores in the ASD group. However, there were some SRS scores that were missed while collecting data from the parents. Therefore, the relationships between the FC of each brain network and clinical symptom scores should be interpreted with caution. Finally, in the imaging genetics analysis conducted in this study, two SNPs were targeted. Nonetheless, as previous research has highlighted the significance of other SNPs of OXTR gene in ASD, it would be valuable to investigate the cumulative or interactive effects of additional SNPs in future studies.

Conclusion

In conclusion, comparing functional brain networks between children with ASD and TD children, children with ASD generally showed under-connectivity than TD

children in brain regions related to higher-order cognitive functions, whereas they showed over-connectivities in brain regions related to lower-level sensory and motor functions. The results of these two opposing directions suggest that brain development in children with ASD undergoes various atypical processes depending on the brain network. Moreover, we observed significant correlations between atypical intrinsic connectivities and clinical scores in children with ASD, and our findings demonstrate that under-/or over-connectivity of each brain region observed in children with ASD plays a role as a bridge to express phenotype.

In addition, through imaging genetic/epigenetic analysis of the OXTR gene, we found that the OXTR caused significant changes in intrinsic brain connectivity of ASD children which distinguished from that of TD children. Since the binding of oxytocin receptors in human brains has been known to be limited to a small number of subcortical regions, previous imaging genetic studies on OXTR have focused on specific brain areas mainly related to the reward circuit, such as NAcc, hypothalamus, amygndala, and etc (123). In this study, we analyzed the entire brain network together using the ICA method, showing that the effects of genetic and epigenetic variants in OXTR can affect a wide variety of brain regions linked to diverse cognitive, social, motor, and sensor functions, rather than being restricted to specific brain areas.

Aberrant intrinsic networks found in children with ASD, which develop in various directions depending on the brain region, can be considered diagnostic tools for ASD. Furthermore, the consistent effect of genetic and epigenetic variations in the OXTR gene on intergroup FC differences across various brain regions displaying atypical connectivity in ASD children, suggests the potential use of imaging genetics

of OXTR as a biomarker for autism. Moreover, this study holds greater significance in that it includes young children with severe symptoms as participants, highlighting the biological characteristics associated with the autistic symptoms found in this study. Further investigation through follow-up studies is warranted to validate the findings of this study in a larger and more stratified population.

Bibliography

1.   Geschwind DH. Genetics of autism spectrum disorders. Trends in Cognitive Sciences. 2011;15(9):409-16.

2.   Goldani AAS, Downs SR, Widjaja F, Lawton B, Hendren RL. Biomarkers in Autism. Frontiers in Psychiatry. 2014;5.

3.   Hus Y, Segal O. Challenges surrounding the diagnosis of autism in children. Neuropsychiatric Disease and Treatment. 2021;17:3509.

4.   Huerta M, Lord C. Diagnostic evaluation of autism spectrum disorders. Pediatric Clinics. 2012;59(1):103-11.

5.   Iidaka T. Resting state functional magnetic resonance imaging and neural network classified autism and control. Cortex. 2015;63:55-67.

6.   Lainhart JE. Brain imaging research in autism spectrum disorders: in search of neuropathology and health across the lifespan. Curr Opin Psychiatry. 2015;28(2):76-82.

7.   Padmanabhan A, Lynn A, Foran W, Luna B, O'Hearn K. Age related changes in striatal resting state functional connectivity in autism. Frontiers in Human Neuroscience. 2013;7(814).

8.   Doyle-Thomas KAR, Lee W, Foster NEV, Tryfon A, Ouimet T, Hyde KL, et al. Atypical functional brain connectivity during rest in autism spectrum disorders. Annals of Neurology. 2015;77(5):866-76.

9.   Monk CS, Peltier SJ, Wiggins JL, Weng S-J, Carrasco M, Risi S, et al. Abnormalities of intrinsic functional connectivity in autism spectrum disorders. Neuroimage. 2009;47(2):764-72.

10.   Dekhil O, Hajjdiab H, Shalaby A, Ali MT, Ayinde B, Switala A, et al. Using resting state functional MRI to build a personalized autism diagnosis system. PLOS ONE. 2018;13(10):e0206351.

11.   Lau WKW, Leung M-K, Lau BWM. Resting-state abnormalities in Autism Spectrum Disorders: A meta-analysis. Scientific Reports. 2019;9(1):3892.

12.   Uddin L, Supekar K, Menon V. Typical and atypical development of functional human brain networks: insights from resting-state fMRI. Frontiers in Systems Neuroscience. 2010;4.

13.   Uddin L, Supekar K, Menon V. Reconceptualizing functional brain connectivity in autism from a developmental perspective. Frontiers in Human Neuroscience. 2013;7(458).

14.   Nair A, Keown CL, Datko M, Shih P, Keehn B, Müller R-A. Impact of methodological variables on functional connectivity findings in autism spectrum disorders. Human Brain Mapping. 2014;35(8):4035-48.

15.   Müller RA, Shih P, Keehn B, Deyoe JR, Leyden KM, Shukla DK. Underconnected, but how? A survey of functional connectivity MRI studies in autism spectrum disorders. Cereb Cortex. 2011;21(10):2233-43.

16.   Hull JV, Dokovna LB, Jacokes ZJ, Torgerson CM, Irimia A, Van Horn JD. Resting-State Functional Connectivity in Autism Spectrum Disorders: A Review. Frontiers in Psychiatry. 2017;7(205).

17.   Braden BB, Smith CJ, Thompson A, Glaspy TK, Wood E, Vatsa D, et al. Executive function and functional and structural brain differences in middle-age adults with autism spectrum disorder. Autism Res. 2017;10(12):1945-59.

18.   Yue X, Zhang G, Li X, Shen Y, Wei W, Bai Y, et al. Abnormal Dynamic

Functional Network Connectivity in Adults with Autism Spectrum Disorder. Clin Neuroradiol. 2022;32(4):1087-96.

19.   Wang K, Xu M, Ji Y, Zhang L, Du X, Li J, et al. Altered social cognition and connectivity of default mode networks in the co-occurrence of autistic spectrum disorder and attention deficit hyperactivity disorder. Aust N Z J Psychiatry. 2019;53(8):760-71.

20.   Lidstone DE, Rochowiak R, Mostofsky SH, Nebel MB. A Data Driven Approach Reveals That Anomalous Motor System Connectivity is Associated With the Severity of Core Autism Symptoms. Autism Res. 2021.

21.   A. Bartz J, Hollander E. The neuroscience of affiliation: Forging links between basic and clinical research on neuropeptides and social behavior. Hormones and Behavior. 2006;50(4):518-28.

22.   MacDonald K, MacDonald TM. The peptide that binds: a systematic review of oxytocin and its prosocial effects in humans. Harvard review of psychiatry. 2010;18(1):1-21.

23.   Ross HE, Young LJ. Oxytocin and the neural mechanisms regulating social cognition and affiliative behavior. Frontiers in Neuroendocrinology. 2009;30(4):534-47.

24.   Campbell DB, Datta D, Jones ST, Batey Lee E, Sutcliffe JS, Hammock EAD, et al. Association of oxytocin receptor (OXTR) gene variants with multiple phenotype domains of autism spectrum disorder. Journal of Neurodevelopmental Disorders. 2011;3(2):101-12.

25.   Kranz TM, Kopp M, Waltes R, Sachse M, Duketis E, Jarczok TA, et al. Meta-analysis and association of two common polymorphisms of the human

oxytocin receptor gene in autism spectrum disorder. Autism Research. 2016;9(10):1036-45.

26.   Liu X, Kawashima M, Miyagawa T, Otowa T, Latt KZ, Thiri M, et al. Novel rare variations of the oxytocin receptor (OXTR) gene in autism spectrum disorder individuals. Human Genome Variation. 2015;2(1).

27.   Fakhoury M. Imaging genetics in autism spectrum disorders: Linking genetics and brain imaging in the pursuit of the underlying neurobiological mechanisms. Progress in Neuro-Psychopharmacology and Biological Psychiatry. 2018;80:101-14.

28.   LoParo D, Waldman ID. The oxytocin receptor gene (OXTR) is associated with autism spectrum disorder: a meta-analysis. Mol Psychiatry. 2015;20(5):640-6.

29.   Tost H, Kolachana B, Hakimi S, Lemaitre H, Verchinski BA, Mattay VS, et al. A common allele in the oxytocin receptor gene (OXTR) impacts prosocial temperament and human hypothalamic-limbic structure and function. Proc Natl Acad Sci U S A. 2010;107(31):13936-41.

30.   Schneider-Hassloff H, Straube B, Jansen A, Nuscheler B, Wemken G, Witt SH, et al. Oxytocin receptor polymorphism and childhood social experiences shape adult personality, brain structure and neural correlates of mentalizing. Neuroimage. 2016;134:671-84.

31.   Inoue H, Yamasue H, Tochigi M, Abe O, Liu X, Kawamura Y, et al. Association Between the Oxytocin Receptor Gene and Amygdalar Volume in Healthy Adults. Biological Psychiatry. 2010;68(11):1066-72.

32.   Furman DJ, Chen MC, Gotlib IH. Variant in oxytocin receptor gene is associated with amygdala volume. Psychoneuroendocrinology. 2011;36(6):891-7.

33.   Tost H, Kolachana B, Verchinski BA, Bilek E, Goldman AL, Mattay VS, et al. Neurogenetic Effects of OXTR rs2254298 in the Extended Limbic System of Healthy Caucasian Adults. Biological Psychiatry. 2011;70(9):e37-e9.

34.   Saito Y, Suga M, Tochigi M, Abe O, Yahata N, Kawakubo Y, et al. Neural correlate of autistic-like traits and a common allele in the oxytocin receptor gene. Social Cognitive and Affective Neuroscience. 2013;9(10):1443-50.

35.   Yamasue H. Function and structure in social brain regions can link oxytocin-receptor genes with autistic social behavior. Brain Dev. 2013;35(2):111-8.

36.   Moerkerke M, Bonte M-L, Daniels N, Chubar V, Alaerts K, Steyaert J, et al. Oxytocin receptor gene (OXTR) DNA methylation is associated with autism and related social traits – A systematic review. Research in Autism Spectrum Disorders. 2021;85:101785.

37.   Maud C, Ryan J, McIntosh JE, Olsson CA. The role of oxytocin receptor gene (OXTR) DNA methylation (DNAm) in human social and emotional functioning: a systematic narrative review. BMC Psychiatry. 2018;18(1):154.

38.   Kraaijenvanger EJ, He Y, Spencer H, Smith AK, Bos PA, Boks MPM. Epigenetic variability in the human oxytocin receptor (OXTR) gene: A possible pathway from early life experiences to psychopathologies. Neuroscience & Biobehavioral Reviews. 2019;96:127-42.

39.   Deaton AM, Bird A. CpG islands and the regulation of transcription. Genes Dev. 2011;25(10):1010-22.

40.   Gregory SG, Connelly JJ, Towers AJ, Johnson J, Biscocho D, Markunas CA, et al. Genomic and epigenetic evidence for oxytocin receptor deficiency in autism. BMC Med. 2009;7:62.

41.   Lord C, Risi S, Lambrecht L, Cook EH, Leventhal BL, DiLavore PC, et al. The Autism Diagnostic Observation Schedule—Generic: A Standard Measure of Social and Communication Deficits Associated with the Spectrum of Autism. Journal of Autism and Developmental Disorders. 2000;30(3):205-23.

42.   Eric Schopler MEVB, Glenna Janette Wellman, Steven R. Love. Childhood Autism Rating Scale – 2nd Edition. Los Angeles: Western Psychological Services; 2010.

43.   Constantino JN. Social Responsiveness Scale. In: Volkmar FR, editor. Encyclopedia of Autism Spectrum Disorders. New York, NY: Springer New York; 2013. p. 2919-29.

44.   Park KS, Yoon YJ, Park HJ, Kwon KU. Korean Educational Development Institute-Wechsler Intelligence scale for children (KEDI-WISC). Seoul: Korean Educational Development Institute; 2002.

45.   Shin MS, Cho S-C. Korean Leiter international performance scale-revised (K-Leiter-R). Seoul: Hakjisa; 2010.

46.   Yan C-G, Wang X-D, Zuo X-N, Zang Y-F. DPABI: Data Processing & Analysis for (Resting-State) Brain Imaging. Neuroinformatics. 2016;14(3):339-51.

47.   Calhoun VD, Adali T, Pearlson GD, Pekar JJ. A method for making group inferences from functional MRI data using independent component analysis. Hum Brain Mapp. 2001;14(3):140-51.

48.   Bell AJ, Sejnowski TJ. An information-maximization approach to blind separation and blind deconvolution. Neural Comput. 1995;7(6):1129-59.

49.   Himberg J, Hyvärinen A, Esposito F. Validating the independent components of neuroimaging time series via clustering and visualization.

Neuroimage. 2004;22(3):1214-22.

50.   Allen E, Erhardt E, Damaraju E, Gruner W, Segall J, Silva R, et al. A Baseline for the Multivariate Comparison of Resting-State Networks. Frontiers in Systems Neuroscience. 2011;5.

51.   Jafri MJ, Pearlson GD, Stevens M, Calhoun VD. A method for functional network connectivity among spatially independent resting-state components in schizophrenia. Neuroimage. 2008;39(4):1666-81.

52.   Just MA, Cherkassky VL, Keller TA, Minshew NJ. Cortical activation and synchronization during sentence comprehension in high-functioning autism: evidence of underconnectivity. Brain. 2004;127(8):1811-21.

53.   Cherkassky VL, Kana RK, Keller TA, Just MA. Functional connectivity in a baseline resting-state network in autism. Neuroreport. 2006;17(16):1687-90.

54.   Kennedy DP, Courchesne E. The intrinsic functional organization of the brain is altered in autism. Neuroimage. 2008;39(4):1877-85.

55.   Jones TB, Bandettini PA, Kenworthy L, Case LK, Milleville SC, Martin A, et al. Sources of group differences in functional connectivity: an investigation applied to autism spectrum disorder. Neuroimage. 2010;49(1):401-14.

56.   Just MA, Keller TA, Malave VL, Kana RK, Varma S. Autism as a neural systems disorder: A theory of frontal-posterior underconnectivity. Neuroscience & Biobehavioral Reviews. 2012;36(4):1292-313.

57.   Weng S-J, Wiggins JL, Peltier SJ, Carrasco M, Risi S, Lord C, et al. Alterations of resting state functional connectivity in the default network in adolescents with autism spectrum disorders. Brain Research. 2010;1313:202-14.

58.   Schipul S, Keller T, Just M. Inter-Regional Brain Communication and Its

Disturbance in Autism. Frontiers in Systems Neuroscience. 2011;5.

59.   Mars RB, Neubert F-X, Noonan MP, Sallet J, Toni I, Rushworth MFS. On the relationship between the "default mode network" and the "social brain". Frontiers in human neuroscience. 2012;6:189-.

60.   Molnar-Szakacs I, Uddin LQ. Self-processing and the default mode network: interactions with the mirror neuron system. Front Hum Neurosci. 2013;7:571.

61.   Li W, Mai X, Liu C. The default mode network and social understanding of others: what do brain connectivity studies tell us. Front Hum Neurosci. 2014;8:74.

62.   Padmanabhan A, Lynch CJ, Schaer M, Menon V. The Default Mode Network in Autism. Biol Psychiatry Cogn Neurosci Neuroimaging. 2017;2(6):476-86.

63.   Utevsky AV, Smith DV, Huettel SA. Precuneus is a functional core of the default-mode network. J Neurosci. 2014;34(3):932-40.

64.   Gusnard DA, Raichle ME. Searching for a baseline: Functional imaging and the resting human brain. Nature Reviews Neuroscience. 2001;2(10):685-94.

65.   Andrews-Hanna JR, Reidler JS, Huang C, Buckner RL. Evidence for the default network's role in spontaneous cognition. J Neurophysiol. 2010;104(1):322-35.

66.   Schilbach L, Eickhoff SB, Rotarska-Jagiela A, Fink GR, Vogeley K. Minds at rest? Social cognition as the default mode of cognizing and its putative relationship to the "default system" of the brain. Conscious Cogn. 2008;17(2):457-67.

67.   Olivito G, Clausi S, Laghi F, Tedesco AM, Baiocco R, Mastropasqua C, et al. Resting-state functional connectivity changes between dentate nucleus and

cortical social brain regions in autism spectrum disorders. The Cerebellum. 2017;16:283-92.

68.   Cheng W, Rolls ET, Gu H, Zhang J, Feng J. Autism: reduced connectivity between cortical areas involved in face expression, theory of mind, and the sense of self. Brain. 2015;138(Pt 5):1382-93.

69.   Fishman I, Keown CL, Lincoln AJ, Pineda JA, Müller R-A. Atypical cross talk between mentalizing and mirror neuron networks in autism spectrum disorder. JAMA psychiatry. 2014;71(7):751-60.

70.   Funakoshi Y, Harada M, Otsuka H, Mori K, Ito H, Iwanaga T. Default mode network abnormalities in children with autism spectrum disorder detected by resting-state functional magnetic resonance imaging. J Med Invest. 2016;63(3-4):204-8.

71.   Lynch CJ, Uddin LQ, Supekar K, Khouzam A, Phillips J, Menon V. Default mode network in childhood autism: posteromedial cortex heterogeneity and relationship with social deficits. Biol Psychiatry. 2013;74(3):212-9.

72.   Yoon N, Huh Y, Lee H, Kim JI, Lee J, Yang CM, et al. Alterations in Social Brain Network Topology at Rest in Children With Autism Spectrum Disorder. Psychiatry Investig. 2022;19(12):1055-68.

73.   Zhang M, Savill N, Margulies DS, Smallwood J, Jefferies E. Distinct individual differences in default mode network connectivity relate to off-task thought and text memory during reading. Scientific Reports. 2019;9(1):16220.

74.   Lombardo MV, Eyler L, Moore A, Datko M, Carter Barnes C, Cha D, et al. Default mode-visual network hypoconnectivity in an autism subtype with pronounced social visual engagement difficulties. eLife. 2019;8:e47427.

75.   Abrams DA, Lynch CJ, Cheng KM, Phillips J, Supekar K, Ryali S, et al.

Underconnectivity between voice-selective cortex and reward circuitry in children with autism. Proceedings of the National Academy of Sciences. 2013;110(29):12060-5.

76.   Watanabe T, Rees G. Brain network dynamics in high-functioning individuals with autism. Nature Communications. 2017;8(1):16048.

77.   Pugliese CE, Anthony L, Strang JF, Dudley K, Wallace GL, Kenworthy L. Increasing adaptive behavior skill deficits from childhood to adolescence in autism spectrum disorder: role of executive function. J Autism Dev Disord. 2015;45(6):1579-87.

78.   Wang Y, Zhang Y-b, Liu L-l, Cui J-f, Wang J, Shum DHK, et al. A Meta-Analysis of Working Memory Impairments in Autism Spectrum Disorders. Neuropsychology Review. 2017;27(1):46-61.

79.   Eigsti I-M, de Marchena AB, Schuh JM, Kelley E. Language acquisition in autism spectrum disorders: A developmental review. Research in Autism Spectrum Disorders. 2011;5(2):681-91.

80.   Mody M, Belliveau JW. Speech and Language Impairments in Autism: Insights from Behavior and Neuroimaging. N Am J Med Sci (Boston). 2013;5(3):157-61.

81.   Haigh SM, Walsh JA, Mazefsky CA, Minshew NJ, Eack SM. Processing Speed is Impaired in Adults with Autism Spectrum Disorder, and Relates to Social Communication Abilities. J Autism Dev Disord. 2018;48(8):2653-62.

82.   Boxhoorn S, Lopez E, Schmidt C, Schulze D, Hänig S, Freitag CM. Attention profiles in autism spectrum disorder and subtypes of attention-deficit/hyperactivity disorder. Eur Child Adolesc Psychiatry. 2018;27(11):1433-47.

83.   Marek S, Dosenbach NUF. The frontoparietal network: function, electrophysiology, and importance of individual precision mapping. Dialogues Clin Neurosci. 2018;20(2):133-40.

84.   May KE, Kana RK. Frontoparietal Network in Executive Functioning in Autism Spectrum Disorder. Autism Research. 2020;13(10):1762-77.

85.   Han YMY, Chan M-C, Chan MMY, Yeung MK, Chan AS. Effects of working memory load on frontal connectivity in children with autism spectrum disorder: a fNIRS study. Scientific Reports. 2022;12(1):1522.

86.   Yerys BE, Tunç B, Satterthwaite TD, Antezana L, Mosner MG, Bertollo JR, et al. Functional Connectivity of Frontoparietal and Salience/Ventral Attention Networks Have Independent Associations With Co-occurring Attention-Deficit/Hyperactivity Disorder Symptoms in Children With Autism. Biol Psychiatry Cogn Neurosci Neuroimaging. 2019;4(4):343-51.

87.   Di Martino A, Kelly C, Grzadzinski R, Zuo X-N, Mennes M, Mairena MA, et al. Aberrant Striatal Functional Connectivity in Children with Autism. Biological Psychiatry. 2011;69(9):847-56.

88.   Cerliani L, Mennes M, Thomas RM, Di Martino A, Thioux M, Keysers C. Increased Functional Connectivity Between Subcortical and Cortical Resting-State Networks in Autism Spectrum Disorder. JAMA Psychiatry. 2015;72(8):767-77.

89.   Woodward ND, Giraldo-Chica M, Rogers B, Cascio CJ. Thalamocortical Dysconnectivity in Autism Spectrum Disorder: An Analysis of the Autism Brain Imaging Data Exchange. Biological Psychiatry: Cognitive Neuroscience and Neuroimaging. 2017;2(1):76-84.

90.   Maximo JO, Kana RK. Aberrant "deep connectivity" in autism: A cortico-

subcortical functional connectivity magnetic resonance imaging study. Autism Res. 2019;12(3):384-400.

91.   Hwang K, Bertolero MA, Liu WB, D'Esposito M. The Human Thalamus Is an Integrative Hub for Functional Brain Networks. J Neurosci. 2017;37(23):5594-607.

92.   Fu Z, Tu Y, Di X, Du Y, Sui J, Biswal BB, et al. Transient increased thalamic-sensory connectivity and decreased whole-brain dynamism in autism. Neuroimage. 2019;190:191-204.

93.   Lorenzini L, van Wingen G, Cerliani L. Atypically high influence of subcortical activity on primary sensory regions in autism. NeuroImage: Clinical. 2021;32:102839.

94.   Supekar K, Musen M, Menon V. Development of Large-Scale Functional Brain Networks in Children. PLOS Biology. 2009;7(7):e1000157.

95.   Nyatega CO, Qiang L, Adamu MJ, Younis A, Kawuwa HB. Altered Dynamic Functional Connectivity of Cuneus in Schizophrenia Patients: A Resting-State fMRI Study. Applied Sciences. 2021;11(23):11392.

96.   Ayub R, Sun KL, Flores RE, Lam VT, Jo B, Saggar M, et al. Thalamocortical connectivity is associated with autism symptoms in high-functioning adults with autism and typically developing adults. Translational Psychiatry. 2021;11(1):93.

97.   Foss-Feig JH, Heacock JL, Cascio CJ. Tactile responsiveness patterns and their association with core features in autism spectrum disorders. Research in Autism Spectrum Disorders. 2012;6(1):337-44.

98.   Cascio CJ, Lorenzi J, Baranek GT. Self-reported Pleasantness Ratings and

Examiner-Coded Defensiveness in Response to Touch in Children with ASD: Effects of Stimulus Material and Bodily Location. J Autism Dev Disord. 2016;46(5):1528-37.

99.   Kirby AV, Little LM, Schultz B, Baranek GT. Observational characterization of sensory interests, repetitions, and seeking behaviors. The American Journal of Occupational Therapy. 2015;69(3):6903220010p1-p9.

100.   Johnson BP, Rinehart NJ, White O, Millist L, Fielding J. Saccade adaptation in autism and Asperger's disorder. Neuroscience. 2013;243:76-87.

101.   Miyahara M, Tsujii M, Hori M, Nakanishi K, Kageyama H, Sugiyama T. Brief report: motor incoordination in children with Asperger syndrome and learning disabilities. J Autism Dev Disord. 1997;27(5):595-603.

102.   Noterdaeme M, Mildenberger K, Minow F, Amorosa H. Evaluation of neuromotor deficits in children with autism and children with a specific speech and language disorder. Eur Child Adolesc Psychiatry. 2002;11(5):219-25.

103.   Tomasi D, Volkow ND. Reduced Local and Increased Long-Range Functional Connectivity of the Thalamus in Autism Spectrum Disorder. Cereb Cortex. 2019;29(2):573-85.

104.   Marandel F, Charrier G, Lamy J-B, Le Cam S, Lorance P, Trenkel VM. Estimating effective population size using RADseq: Effects of SNP selection and sample size. Ecology and Evolution. 2020;10(4):1929-37.

105.   Dennis EL, Jahanshad N, Rudie JD, Brown JA, Johnson K, McMahon KL, et al. Altered structural brain connectivity in healthy carriers of the autism risk gene, CNTNAP2. Brain connectivity. 2011;1(6):447-59.

106.   Whalley HC, O'Connell G, Sussmann JE, Peel A, Stanfield AC, Hayiou-

Thomas ME, et al. Genetic variation in CNTNAP2 alters brain function during linguistic processing in healthy individuals. Am J Med Genet B Neuropsychiatr Genet. 2011;156b(8):941-8.

107.　　Hernandez LM, Krasileva K, Green SA, Sherman LE, Ponting C, McCarron R, et al. Additive effects of oxytocin receptor gene polymorphisms on reward circuitry in youth with autism. Mol Psychiatry. 2017;22(8):1134-9.

108.　　Wang J, Braskie MN, Hafzalla GW, Faskowitz J, McMahon KL, de Zubicaray GI, et al. Relationship of a common OXTR gene variant to brain structure and default mode network function in healthy humans. Neuroimage. 2017;147:500-6.

109.　　Gimpl G, Fahrenholz F. The oxytocin receptor system: structure, function, and regulation. Physiol Rev. 2001;81(2):629-83.

110.　　Uzefovsky F, Bethlehem RAI, Shamay-Tsoory S, Ruigrok A, Holt R, Spencer M, et al. The oxytocin receptor gene predicts brain activity during an emotion recognition task in autism. Molecular Autism. 2019;10(1):12.

111.　　Wang J, Qin W, Liu B, Wang D, Zhang Y, Jiang T, et al. Variant in OXTR gene and functional connectivity of the hypothalamus in normal subjects. Neuroimage. 2013;81:199-204.

112.　　Zeev-Wolf M, Levy J, Ebstein RP, Feldman R. Cumulative Risk on Oxytocin-Pathway Genes Impairs Default Mode Network Connectivity in Trauma-Exposed Youth. Front Endocrinol (Lausanne). 2020;11:335.

113.　　Puglia MH, Connelly JJ, Morris JP. Epigenetic regulation of the oxytocin receptor is associated with neural response during selective social attention. Translational Psychiatry. 2018;8(1):116.

114.   Andari E, Nishitani S, Kaundinya G, Caceres GA, Morrier MJ, Ousley O, et al. Epigenetic modification of the oxytocin receptor gene: implications for autism symptom severity and brain functional connectivity. Neuropsychopharmacology. 2020;45(7):1150-8.

115.   Mao D, Ding Z, Jia W, Liao W, Li X, Huang H, et al. Low-Frequency Fluctuations of the Resting Brain: High Magnitude Does Not Equal High Reliability. PLOS ONE. 2015;10(6):e0128117.

116.   Duff EP, Johnston LA, Xiong J, Fox PT, Mareels I, Egan GF. The power of spectral density analysis for mapping endogenous BOLD signal fluctuations. Human Brain Mapping. 2008;29(7):778-90.

117.   Lewis LD, Setsompop K, Rosen BR, Polimeni JR. Fast fMRI can detect oscillatory neural activity in humans. Proceedings of the National Academy of Sciences. 2016;113(43):E6679-E85.

118.   Kajimura S, Margulies D, Smallwood J. Frequency-specific brain network architecture in resting-state fMRI. Scientific Reports. 2023;13(1):2964.

119.   Calhoun V, Sui J, Kiehl K, Turner J, Allen E, Pearlson G. Exploring the Psychosis Functional Connectome: Aberrant Intrinsic Networks in Schizophrenia and Bipolar Disorder. Frontiers in Psychiatry. 2012;2.

120.   Agcaoglu O, Wilson TW, Wang YP, Stephen JM, Fu Z, Calhoun VD. Altered resting fMRI spectral power in data-driven brain networks during development: A longitudinal study. J Neurosci Methods. 2022;372:109537.

121.   Liu X, Lauer KK, Douglas Ward B, Roberts C, Liu S, Gollapudy S, et al. Propofol attenuates low-frequency fluctuations of resting-state fMRI BOLD signal in the anterior frontal cortex upon loss of consciousness. Neuroimage.

2017;147:295-301.

122.   Di Francesco MW, Robertson SA, Karunanayaka P, Holland SK. BOLD fMRI in infants under sedation: Comparing the impact of pentobarbital and propofol on auditory and language activation. Journal of Magnetic Resonance Imaging. 2013;38(5):1184-95.

123.   Freeman SM, Palumbo MC, Lawrence RH, Smith AL, Goodman MM, Bales KL. Effect of age and autism spectrum disorder on oxytocin receptor density in the human basal forebrain and midbrain. Transl Psychiatry. 2018;8(1):257.

국문 초록

배경 및 목적: 자폐스펙트럼장애의 다양한 특성들과 옥시토신수용체 유전자와의 관련성이 알려져 있으며, 최근 연구들에서는 옥시토신수용체 유전자의 다형성이 자폐스펙트럼장애 아동의 뇌 기능적 네트워크에 영향을 미칠 가능성을 제안하였다. 그러나 뇌 영역별 기능적 연결성에 대한 기존 연구 결과는 일관되지 않으며, 특히 어린 자폐증 아동에서는 옥시토신수용체 유전자와 뇌 기능적 연결성의 관계에 대해 잘 알려지지 않았다. 본 연구에서는 학령전기를 포함한 중증의 자폐스펙트럼장애 아동에서 휴식기 뇌 기능적 연결성의 특징을 확인하고, 정상 발달 아동과 구분되는 자폐스펙트럼장애 아동의 특징적 뇌 기능적 연결성에 대한 옥시토신수용체 유전자의 영향을 탐색하고자 하였다.

방법: 본 연구는 2세에서 12세 사이의 43명의 자폐스펙트럼장애 아동 및 54명의 정상 발달 아동을 대상으로 하였다. 혈액 검사를 통하여 옥시토신수용체 유전자에서 두 개의 단일 염기 다형성 (SNP) 데이터와 DNA 메틸화 데이터를 얻었고, 휴식기 기능적 자기공명 영상을 이용하여 뇌 영상 데이터를 수집하였다. 우리는 독립 성분 분석 방법으로 뇌 영역을 6가지 고유 네트워크로 분류하였고, 각 네트워크의 기능적 연결성을 산출하여 두 군간에 유의미한 차이를 확인하였다. 그 후, 옥시토신수용체 유전자와 진단 간 상호작용 효과를 분석하였다. 통계적으로 유의미한 결과를 보인 네트워크에 대하여 기능적 연결성과 자폐증의 임상 증상 점수 간의 상관 관계를 분석하였다.

결과: 자폐스펙트럼장애 아동은 정상 발달 아동에 비하여 cognitive

control network, default mode network, visual (VIS) network, somatomotor (SM) network에서 기능적 연결성이 저하된 반면, subcortical network, VIS, SM network에서는 과연결성 (over-connectivity)이 관찰되었다. 그리고 이러한 비정상적인 기능적 연결성은 자폐증 임상 점수와 유의미한 상관성을 보였다. 기능적 연결성에 대한 옥시토신수용체 유전자의 영향을 살펴보았을 때, 두 개의 SNP (rs2254298과 rs53576)의 위험 대립유전자와 관련하여, 대부분의 내재적 뇌 연결성은 자폐스펙트럼장애 그룹에서 감소하고 정상 발달 그룹에서 증가함으로써, 결과적으로 두 그룹 간의 기능적 연결성의 차이가 유의미하게 커졌다. 반면, subcortico-cortical network에 관련된 일부 연결에서는 자폐 아동에서 연결성이 증가하고 정상 발달 아동에서는 감소하였으나, 마찬가지로 두 그룹 간의 대조는 더욱 커지는 결과를 보였다. 후성유전학적 분석에서는 옥시토신수용체 유전자의 메틸화 증가가 두 그룹 간의 기능적 연결성 차이에 유의미한 영향을 미치는 것을 발견하였다. 옥시토신수용체 유전자의 유전형에 따라 유의미한 변화가 발견된 network에서 임상적 상관성을 발견하였으나, 후성유전학적 영상 분석에서는 임상적 상관성을 보이지 않았다. Spectra 분석 결과, 저주파 영역에서는 정상 발달 아동이 자폐 아동에 비하여 더 큰 값을 보였고, 고주파 영역에서는 자폐 아동의 spectral power가 더 강하였다. 옥시토신수용체 유전자와 관련하여 spectral power를 분석한 결과도 이와 유사하였다.

결론: 본 연구 결과, 자폐스펙트럼장애 아동에서 휴식기 뇌 기능적 연결성은 뇌 영역에 따라 다양하게 관찰되며, 이러한 뇌 기능적 연결성의 이상은 정상 발달 아동과 구분되는 특징으로써 자폐스펙트럼장애 진단의 생물학적 기초가 될 수 있다. 또한 본

연구에서는 옥시토신수용체 유전자의 유전학적, 후성유전학적 다양성이 자폐스펙트럼 장애의 비정상적인 뇌 기능적 연결성에 일관된 영향을 미치는 것을 확인하였고, 따라서 옥시토신수용체 유전자를 활용한 영상 유전학적, 영상 후성유전학적 특징이 자폐스펙트럼장애의 바이오마커로 활용될 수 있음을 제시하였다.

주요어: 자폐스펙트럼장애, 옥시토신수용체 유전자, 영상 유전학, 영상 후성유전학, 휴식기 뇌기능자기공명영상, 독립성분분석